

5-2013

Bioelectrochemical Reduction Of Carbon Dioxide To Acetate Using A Microbial Consortium Derived From The Cow Rumen

Ryan Hammonds

Clemson University, rehammo@clemson.edu

Follow this and additional works at: https://tigerprints.clemson.edu/all_theses

 Part of the [Microbiology Commons](#)

Recommended Citation

Hammonds, Ryan, "Bioelectrochemical Reduction Of Carbon Dioxide To Acetate Using A Microbial Consortium Derived From The Cow Rumen" (2013). *All Theses*. 1578.

https://tigerprints.clemson.edu/all_theses/1578

This Thesis is brought to you for free and open access by the Theses at TigerPrints. It has been accepted for inclusion in All Theses by an authorized administrator of TigerPrints. For more information, please contact kokeefe@clemson.edu.

**BIOELECTROCHEMICAL REDUCTION OF CARBON DIOXIDE TO ACETATE
USING A MICROBIAL CONSORTIUM DERIVED FROM THE COW RUMEN**

A Thesis
Presented to
the Graduate School of
Clemson University

In Partial Fulfillment
of the Requirements for the Degree
Master of Science
Microbiology

by
Ryan Everett Hammonds
May 2013

Accepted by:
Dr. J. Michael Henson, Committee Chair
Dr. Tamara L. McNealy
Dr. Stephen E. Creager

ABSTRACT

Pure cultures of chemoautotrophic microorganisms have previously been reported to produce acetate from carbon dioxide using reductive electric current. We hypothesized that electrofuel precursors could be produced in a similar manner from a consortium consisting of microbial populations acting as a stable community. This approach might offer improved efficiency and selectivity, greater sustainability, a more diverse group of end products, and more opportunities for community optimization in electrofuel production than is possible with pure cultures. To evaluate this concept, bovine rumen contents were enriched for autotrophic, anaerobic microbes for several generations using hydrogen and carbon dioxide for growth and energy. A stable acetogenic consortium was obtained and aliquots were transferred to the cathode compartments of bioelectrosynthesis cells with reductive electric current supplied to a biocathode by a potentiostat. Current uptake and biofuel precursor production were simultaneously measured over time for periods lasting from several days to several months. Acetate production rates near 3 millimoles per liter of biocathode volume per day were obtained. To evaluate that acetate production was derived solely from bioelectrochemical reduction of carbon dioxide a series of isotopic labeling experiments was performed. Growth medium was prepared using bicarbonate enriched with ten mole percent of ^{13}C -labeled sodium bicarbonate. The $^{13}\text{C}/^{12}\text{C}$ isotopic ratios in acetate produced by the consortium growing only when current was provided were found by GC-MS analysis to be consistent with the expectation for acetate production from a carbon source (carbon dioxide or bicarbonate) that contained ten mole percent of a ^{13}C label. This finding supports the hypothesis that acetate production in these bioelectrochemical cells is solely the result of microbial-catalyzed bioelectrochemical reduction of carbon dioxide / bicarbonate.

DEDICATION

This work is dedicated to my parents, Bruce and Anne Hammonds.

ACKNOWLEDGMENTS

I would like to thank my advisor, Dr. J. Michael Henson, for his continued support, advice, encouragement, and guidance. I am very grateful to my committee members: Dr. Stephen Creager and Dr. Tamara McNealy for their guidance, input, and advice.

I would also like to thank the contribution and assistance of Dr. Kristi Whitehead and Dr. Jung Min Oh for countless hours of assistance, expertise, and support, Dr. Nashanth Tharayil for assistance and guidance in the MUAL and assistance with GC-MS, and Dr. Terri Bruce for her assistance in the Clemson Light Imaging Facility.

Additionally, I would like to thank my lab mates, Sandra Bediako, Megan Burdette, and Abhiney Jain for helpful discussions, shared knowledge, support, and laughter. Finally, I would like to acknowledge the contribution and assistance of undergraduate workers Jerrie Onley, William Smith, and Yi Jie Wang, for countless hours of assistance.

TABLE OF CONTENTS

	Page
TITLE PAGE	i
ABSTRACT	ii
DEDICATION	iv
ACKNOWLEDGMENTS	v
LIST OF TABLES	vi
LIST OF FIGURES	vii
CHAPTER	
I. INTRODUCTION	1
II. MATERIALS AND METHODS	15
Environmental Sampling	15
Medium Composition and Growth Conditions	16
Microbial Electrosynthesis Cell Design and Operation	17
Consortium Analysis.....	21
Analytical Methods	23
III. RESULTS	25
IV. DISCUSSION	50
REFERENCES	57

LIST OF TABLES

Table		Page
3.1	Sources and results of acetogenic enrichment from several different environments	25
3.2	Predicated and measured peak intensity of acetate fragments of ¹³ C enriched and unenriched MEC systems	36

LIST OF FIGURES

Figure	Page
1.1 The Wood- Ljungdahl pathway for the autotrophic production of acetate from CO ₂ and H ₂	8
1.2 Proposed mechanisms of ATP production during autotrophic growth utilizing the Wood-Ljungdahl pathway	10
2.1 Microbial electrosynthesis cell (MEC) design and construction.....	17
3.1 Acetate production per enrichment generation of Salt Marsh 1 consortium grown in enrichment conditions on H ₂ and CO ₂	26
3.2 Acetate production per enrichment generation of Cow Rumen 1 consortium grown in enrichment conditions on H ₂ and CO ₂	26
3.3 Cumulative electrochemical acetate production of Salt Marsh 1 consortium grown at -590 mV	28
3.4 Cumulative current consumption and coulombic efficiency of Salt Marsh 1 grown at -590 mV	28
3.5 Measured cathode compartment pH of Salt Marsh 1 grown at -590 mV	29
3.6 Cumulative electrochemical acetate production of Cow Rumen 1 consortium grown at -790 mV	30
3.7 Cumulative current consumption and coulombic efficiency of Cow Rumen 1 grown at -790 mV.....	30
3.8 Measured cathode compartment pH of Cow Rumen 1 grown at -790 mV	31
3.9 Quantification of abiotic hydrogen production rates for MEC systems operated at -790 mV.....	32

List of Figures (Continued)

Figure	Page
3.10 Cumulative current consumption and coulombic efficiency for abiotic hydrogen production in a MEC system operated at -790 mV	33
3.11 Evaluation of acetate production of Cow Rumen 1 consortium grown in enrichment conditions at varying pH levels	34
3.12 Mass spectrum profile of electrosynthetic acetate production of Cow Rumen 1 consortium grown on un-supplemented bicarbonate growth medium.....	35
3.13 Mass spectrum profile of electrosynthetic acetate produced of Cow Rumen 1 consortium grown on carbonate supplemented with 10 Mol percent ¹³ C.....	36
3.14 Cyclic voltammetry scan of an abiotic MEC cathode immersed in sterile growth medium	37
3.15 Cyclic voltammetry scan of a MEC cathode colonized by the electroacetogenic Cow Rumen 1 consortium immersed in sterile growth medium.	38
3.16 Scanning electron micrograph of Cow Rumen 1 consortium colonized cathode poised at -790 mV	39
3.17 Scanning electron micrograph of Cow Rumen 1 consortium colonized cathode poised at -790 mV	40
3.18 Scanning electron micrograph of a sterile abiotic cathode poised at -790 mV	41
3.19 Relative abundance of active members of the cathode supernatant consortium of Cow Rumen 1 grown at -790 mV	42
3.20 Acetate production from consortium subsets of Cow Rumen 1 grown on CO ₂ and H ₂	44

List of Figures (Continued)

Figure	Page
3.21 Denaturing gradient gel electrophoresis gel showing total diversity of subsets of the Cow Rumen 1 consortium	45
3.22 Cumulative electrochemical acetate production of Cow Rumen consortium subset 1B CR 10^{-6} grown at -790 mV	46
3.23 Cumulative current consumption and coulombic efficiency of Cow Rumen consortium subset 1B CR 10^{-6} grown at -790 mV	47
3.24 Cumulative electrochemical acetate production of Cow Rumen consortium 1 grown in the presence and absence of an applied potential of -790 mV	48
3.25 Cumulative current consumption and coulombic efficiency of Cow Rumen consortium grown in the presence and absence of an applied potential of -790 mV	49

CHAPTER ONE

INTRODUCTION

Overview

During the twentieth century, the human population nearly quadrupled in size (Roberts, 2011). The large increase in population and the concomitant increase in industrialization around the world required primary power consumption, defined as power produced from non-renewable sources, to have increased tremendously (BP 2012). In 2011 alone, the United States of America consumed over 78 quadrillion British Thermal Units (quads) of energy (US EIA 2013). Of the total energy consumed by the U.S, less than 9 percent was produced by renewable means as of 2011 (US EIA 2013). As such, now more than ever a sustainable source of energy is needed to supplement global fossil fuel consumption. This need is especially true in the United States, which is looking for sustainable sources of domestic energy.

While many green energy alternatives are starting to gain traction in the United States, their inconsistent nature remains a concern (Hoffert et al., 2002). Additionally, the possible disconnect between the timeliness of peak energy production and peak energy demand poses another barrier to widespread implementation. As a result, during times of high-energy output and low-energy demand, storage of excess energy is required. Currently, there are many traditional means of storing excess power, such as batteries or pump storage of water, these solutions are not ideal as they are not well suited for widespread distribution to population centers. The distribution of stored energy is important to the implementation of green energy as areas of the United States most suitable for implementation of energy alternatives typically do not have a nearby population base to consume the power produced. One solution to this problem is to implement appropriate methods of storing excess electrical energy so that it can be easily transported and distributed to locations of high demand.

A possible method to store excess electrical energy is to convert it into a more stable form such as molecules containing carbon-carbon bonds. This method is attractive because of the increased energy storage capacity in these molecules and the current usage of fossil fuels that are composed of carbon-to-carbon bonds. Present research to develop this technology is based on the conversion of electrical current to

reduced end products and is centered on the use of several pure cultures of *Bacteria*. Pure cultures often are not robust enough for large-scale industrial processes for production of transportation fuels; therefore, this project evaluated a mixed microbial community to develop a microbial consortium suited for production of biofuels. In addition, this research project examines the interactions between the various members of the mixed microbial consortium. These cooperative interactions, which to the best of our knowledge are unstudied, enable the consortium to produce end products at a higher rate than that of published pure cultures. Results of this research could provide valuable insight into the design of future consortia to improve the process for storage of excess energy in microbiologically produced multi-carbon molecules.

Members of the biological world, from microbes to humans, spend their lives cycling electrons from donor molecules to acceptor molecules in the process of cellular metabolism. Sources of electrons include carbohydrates, proteins, or lipids as well as inorganic molecules (Gerhard, 1986). These electrons are utilized in the production of energy and the reduction processes that produce cellular biomass. Without the cyclic flow of electrons, the metabolic processes come to a halt. The production of energy is dependent on the difference in potential between the electron donor and acceptor. Thus, humans and many bacteria transfer electrons to oxygen as the terminal electron acceptor for energy production. Anaerobic bacteria, however, transfer electrons to numerous electron acceptors besides oxygen for metabolic processes including nitrogen fixation, fermentation, and carbon dioxide reduction (Gerhard, 1986). These processes require large inputs of electrons (donors) and they yield electron dense products as well. The ability of microbes to funnel electrons from external sources, pass them through membrane bound cytochromes, produce ATP, and eventually pass these electrons to terminal electron acceptors, is by no means a new observation in the field of microbiology. In fact, early characterizations of cytochromes, referred to then as respiratory pigments, were made as early as the late eighteenth century (Hawthorne et al., 1939). While our understanding of microbial cycling of electrons has grown by orders of magnitude since then, it wasn't until recently that there has been a new wave of intense interest in the microbial cycling of electrons. Much of the attention has been focused around the microbial oxidation and reduction of electrodes poised at varying electrochemical potentials. (Nevin et al., 2010) (Nevin et al., 2011) (Ahn et al., 2010) (Kiely 2011)

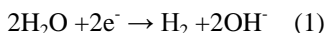
The ability for microbes to interact with poised electrodes has led to many new technologies that could revolutionize the way we live. Electrical energy production from renewable biomass (Deng et al., 2010), desalinization of marine water coupled to energy production (Mehanna et al., 2010), waste water treatment coupled to energy production (Ahn 2010), and the production of biofuel precursors coupled to the sequestration of carbon dioxide (Nevin et al., 2010) (Nevin et al., 2011) (Marshall et al., 2012) are all based on microbe electrode interactions. This literature review will focus on the production of biofuel precursors coupled to the sequestration of carbon dioxide by autotrophic microorganisms.

At its most basic level, the production of biofuel precursors coupled to the sequestration of carbon dioxide is the ability of autoelectrotrophic microbes to utilize electrons taken from an electrode as a source of reducing power in order to reduce carbon dioxide to acetyl-CoA or acetate. Because acetyl-CoA represents a central point in the metabolism of most bacteria, there exists the ability to connect the production of acetyl-CoA by autoelectrotrophic organisms to the metabolism of other microbes to produce a wide range of industrially relevant end products. The ability to oxidize an electrode poised at reducing potentials will circumvent the need for the addition of hydrogen or other costly commodity chemicals that traditionally serve as electron donors (Nevin et al., 2010). More importantly, electrons can easily be derived from renewable energy technologies such as wind and solar power and used to store excess energy produced in the form of molecules comprised of multiple carbon-carbon bonds and possible liquid fuels. This microbial capability addresses many of the current challenges facing the renewable energy field: production timeliness, production location, and energy transportation and distribution.

Extracellular Electron Transfer:

The primary challenge facing microbial electrosynthesis cell (MEC) technology is getting electrons into microbes in quantities sufficient for production of products at levels suitable to industry. To date, three possible mechanisms by which electrotrophic microbes obtain reducing equivalents have been proposed, and these include the electrolysis of water, production of soluble electron mediators, and/or direct electron transfer.

The most fundamental means of shuttling electrons from a reductive cathode is through the direct electrolysis of water to produce hydrogen gas. With a cathode poised at sufficiently low potentials, a reduction will occur via the donation of cathodic electrons to water to form hydrogen gas by the following equation:



Since hydrogen is used as an electron donor by a very large diversity of organisms, hydrogen produced via electrolysis represents a means of shuttling electrons to microbes as demonstrated by Schlegel et al., (Schlegel 1965). At potentials as low as -5.5V, Schlegel achieved good growth of *Pseudomonas hydrogenomonas* reporting that hydrogen could be produced at platinum electrodes and readily consumed by the microorganism. Based on these findings, others have further investigated electrolysis of water and found that it could easily be coupled to other metabolic processes (Kuroda et al., 1996) (Thrash et al., 2008). Of particular interest in this work was the observation that continuous cultures of denitrifying systems would eventually produce biofilm growth associated with the cathode as visualized with scanning electron microscopy (SEM) (Sakakibara 1993). While direct electrolysis of water to hydrogen gas is an effective means of introducing reducing equivalents to microbes grown in association with a cathode, there are two major drawbacks. First, the production of hydrogen by standard carbon electrodes occurs at a large overpotential requiring large energy input for production. Secondly, even if hydrogen could be produced at high potentials, the low aqueous solubility of hydrogen determined by Henry's Law would limit electron availability in solution (Krichevsky et al., 1935).

The discussion of electron transfer up to this point has not centered on a true biotic mechanisms, rather an abiotic electrochemically driven means of producing reducing equivalents suitable for microbial consumption. The following discussions, however, will address various microbial mechanisms that can be referred to as extracellular electron transfer (EET). EET is defined as the ability of microorganisms to utilize an insoluble electron donor or acceptor external to the cell (Hernandez et al., 2001). One approach of shuttling electrons to microbes that may be better suited to use in industrial applications is the use of electron shuttles (Marsili et al., 2008). Electron shuttles are electro active molecules that microbes can

reduce or oxidize without consuming the molecule. In this manner, an oxidized electron shuttle can diffuse to an electrode where it is reduced and becomes available to serve as an electron donor for various microbes. As such, soluble mediators remove the necessity of direct contact between microbes and electrodes.

Electron shuttles are nearly as diverse as the microbes that utilize them. Methyl viologen (Aulenta et al., 1999), flavins (Von Canstein et al., 2008) cobalt sepulchrate (Emde et al., 1990), neutral red (Park et al., 1999), and anthraquinone-2,6-disulfonate (Thrash et al., 2007) have all been demonstrated as soluble electron donors used by microorganisms. While many previous research findings have shown the effectiveness of soluble electron shuttles, there are several disadvantages. Many of the most well characterized soluble electron mediators are highly toxic to microorganisms. Methyl viologen and neutral red, for example, have well documented impacts upon bacterial viability (Park et al., 1999). Secondly, there exists a diffusional limitation, which could impact rates of production formation (Thrash et al., 2008). Finally, the addition of large volumes of electron mediator to industrial systems is impractical and costly; thus, microbial communities would have to be engineered to produce their own mediators, representing a loss of efficiency in electron and carbon input with regards to product formation. Fortunately, there are more direct means of transferring electrons to microbes.

The previous two methods of electron transfer have focused on a mediator, either hydrogen or a soluble molecule, to convey electrons to microbes growing in loose association with a cathode. While the use of electron mediators to eliminate the requirement for direct electrode contact might expand the range of microbes capable of interactions with electrodes, there exists a more direct and efficient way of passing reducing equivalents to microbes. Direct electron transfer relies on a direct contact between an electrode and microbes, either through outer membrane proteins (Lovley, 2012) or conductive appendages (Reguera et al., 2005). This concept was first demonstrated utilizing a pure culture, *Geobacter metallireducens*, grown in direct association with a cathode and reducing nitrate to nitrite (Gregory et al., 2004). These experiments demonstrated that electrons were passed directly from the electrode surface to *G. metallireducens*. Subsequent research has suggested that this method of electron transfer occurs in several

other systems, including *Anaeromyxobacter dehalogenans* (Strycharz et al., 2010), *Geobacter lovleyi* (Strycharz et al., 2008), and *Sporomusa ovata* (Nevin et al., 2010).

While the mechanistic study of direct electron transfer is in its infancy, much of what we know is from the study of conductive appendages of *Geobacter* sp. *Geobacter* sp were first targeted for further study when it was observed that the anodes of sediment-based biological batteries were dominated by species in the *Geobacter* genus (Bond et al., 2002). Subsequent work based on this observation demonstrated that pure cultures of these organisms could support growth by passing electrons from oxidized organics to the surface of graphite electrodes (Bond and Lovley, 2003). High correlations between PilA expression levels and biofilm conductivity led research to further examine the role of pili in direct electron transfer to insoluble substrates (Childers et al., 2002). *Geobacter* sp. with PilA gene knockouts demonstrated complete inhibition of the ability to interact with Fe(III), further implicating its importance in EET (Reguera et al., 2005). Atomic force microscopy of purified PilA later revealed not only that the pili were conductive, but that c-type cytochromes and other redox-active moieties were not responsible for long range electron transfer to electrodes (Reguera et al., 2005). Interestingly, c-type cytochromes do however play a crucial role in the transfer of electrons from insoluble iron (Lovley and Mester, 2008).

Electroacetogenesis:

The reported growth of the acetogen *Sporomusa ovata* in a cathode-associated biofilm is unique in that it was the first reported incidence of autotrophic growth by consuming electrons directly from an electrode in a MEC system (Nevin et al., 2010). Consumption of carbon dioxide and electrical current resulted in the production of acetate and 2-oxybutyrate at cathode potentials of -400 mV versus standard hydrogen electrode (SHE). Following their initial work with *S. ovata*, Nevin et al. (2011) reported similar finding in other acetogenic bacteria including two *Sporomusa* spp., *Clostridium ljungdahlii*, *C. aceticum*, *Moorella thermoacetica*, and *Acetobacterium woodii* observing the bioelectrosynthetic production of acetate, 2-oxobutyrate, and occasionally formate. Several of the species studied were capable of electron recovery efficiencies in excess of 80% (Nevin et al., 2011). As before, each pure culture was found to grow

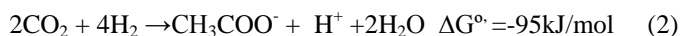
in close association with the cathode in the form of a biofilm and direct electron transfer was the proposed mechanism of electron consumption (Nevin et al., 2010, Nevin et al., 2011).

Until recently, the microbially-catalyzed electrode-dependent reduction of carbon dioxide into higher molecular weight reduced organic compounds focused on pure cultures. However, recent interest in a more diverse range of end products has led to the examination of mixed microbial communities as biocatalysts for the electrosynthetic reduction of carbon dioxide. Recently, the coincident production of acetate, methane, and hydrogen production at a cathode potential of -590 mV using a mixed microbial community derived from brewery waste and grown on granular carbon electrodes has been reported (Marshall et. al., 2012). Following the addition of bromoethanesulphonic acid, they reported acetate and hydrogen as the sole end products.

Acetogens:

Each year more than an estimated one hundred billion tons of acetic acid is produced by microbes (Drake, 1994)). Though heterotrophic fermentation of carbohydrates to acetate is the most often thought of means of acetate production, acetogenic bacteria are capable of producing acetate through the anaerobic respiration of carbon dioxide. Acetogens are a highly diverse group of obligate anaerobic organisms composed of more than twenty-two genera, most of which belong to the phylum Firmicutes (Ragsdale and Pierce, 2008). To date, over one hundred species have been isolated from a diversity of environments including the intestinal tracts of various animals (Joblin, 1999), termites (Breznak, 1994), marine sediments (Liu and Suflita, 1993), and freshwater sediments (Jones and Simon, 1985).

Acetate is produced by acetogens through the Wood-Ljungdahl or reductive acetyl-CoA pathway (Drake, 1994). Acetate or Acetyl-CoA produced via this pathway is the primary means of synthesis of cell carbon for acetogens (Müller et al., 2004). As indicated previously, acetogens are also capable of the fermentation of carbohydrates to form acetate. This review, however, will focus on the anaerobic respiration of carbon dioxide (Equation 2).



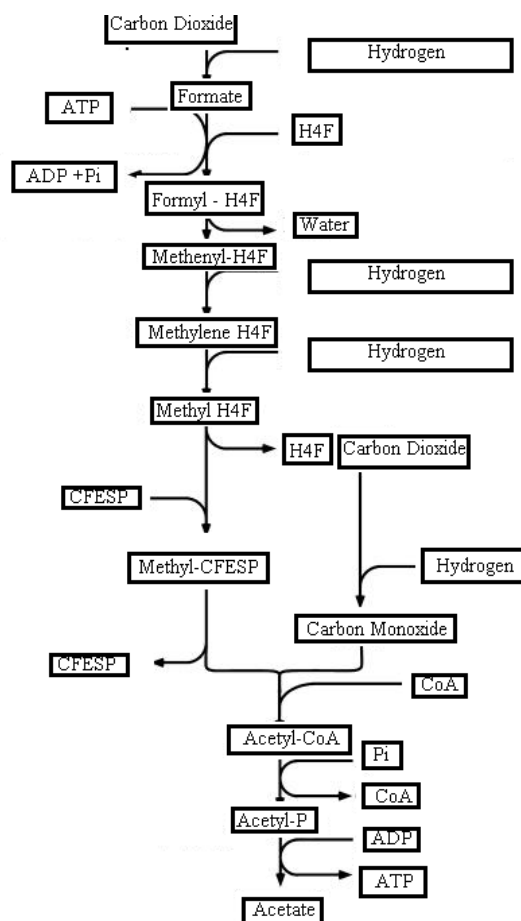


Figure 1.1: The Wood- Ljungdahl pathway for the autotrophic production of acetate from CO_2 and H_2

Energetics:

As shown in equation 2 and **figure 1.1**, the Wood-Ljungdahl pathway involves the reduction of two moles of CO₂ to form acetate (Drake, 1994). Reducing equivalents for this reaction are provided from hydrogen or reductive current as reviewed earlier. The net result of equation 2 is the production of one mole of acetic acid, one mole of protons, and two moles of water. In addition to these products, one mole of ATP is produced via substrate level phosphorylation in the acetate kinase reaction; however, one mole of ATP is also consumed to catalyze the conversion of formate to formyl-H₄F as shown in **Figure 1.1**. With a net ATP output of zero, in order for acetogens to grow chemolithoautotrophically, another means of energy production must be utilized. Fortunately, understanding more about the energetics of acetogens has been the target of a great amount of research in recent years. Acetogens can be characterized into two primary groups depending on the mechanism utilized to produce ATP, H⁺ dependent and Na⁺ dependent acetogens (Ljungdahl, 1994) (Müller and Gottschalk, 1994). Both groups of organisms use phosphorylation mediated by ion gradients: the H⁺ dependent acetogens contain cytochromes and a membrane bound H⁺ motive electron transport chain; while the Na⁺ dependent acetogens lack cytochromes but utilize membrane bound corrinoids to translocate sodium ions (Ljungdahl, 1994) (Müller and Gottschalk, 1994).

The current understanding of H⁺ dependent acetogenic energy conservation began with the purification of multiple membrane-integral electron carriers involved in the electron transport from a model acetogen, *Morella thermoacetica* (Gottwald et al., 1975). Purification of *M. thermoacetica* membranes yielded four primary integral membrane electron carriers: Menaquinone MK-7, two c-type cytochromes, and a flavoprotein (Gottwald et al., 1975). While these proteins were certainly capable of passing electrons through the membranes of H⁺ dependent acetogens, it was unclear whether they could accept electrons from internal electron shuttles. Further preparations of inside out vesicles demonstrated that some enzymes, such as the electron donors CO dehydrogenase, NADH hydrogenase, hydrogenase, and the electron acceptor methylene-H₄F reductase, were capable of attaching to the cytoplasmic membrane (Hugenholtz et al., 1989) These findings led to a proposed energetic mechanism that began with an electron donor such as CO dehydrogenase, NADH dehydrogenase, or hydrogenase, and would terminate with membrane bound

electron carriers such as Methylene H_4F reductase (Hugenholtz et al., 1989). Ultimately, this proposed mechanism would result in ATP synthesis driven by a transmembrane protein potential as seen in Figure 1.2 Though direct evidence for this pathway has yet to be produced, several more recent studies involving artificially produced membrane vesicles have quantified the production of an electrochemical potential resulting from the oxidation of carbon monoxide by CODH (Hugenholtz et al., 1987).

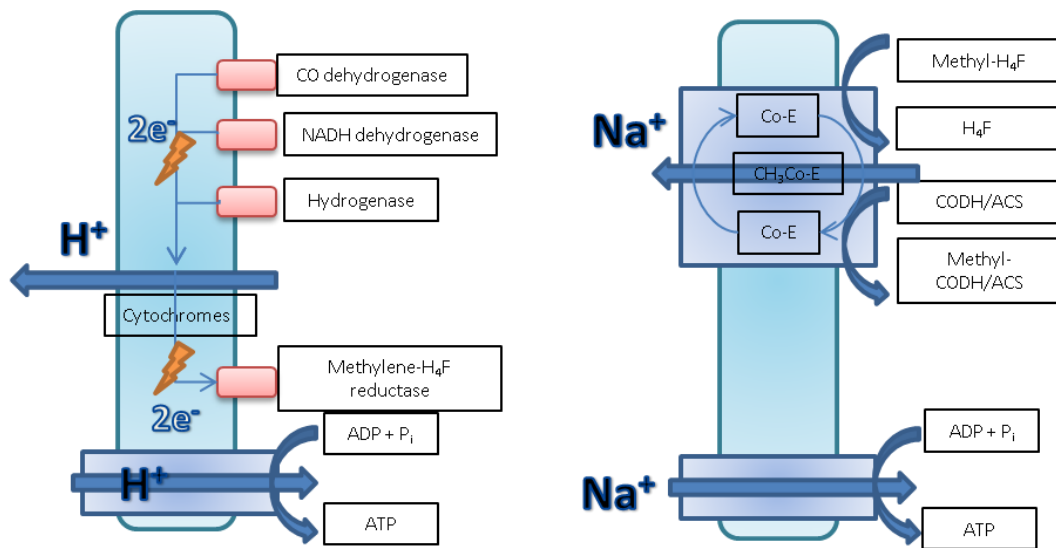


Figure 1.2 : Proposed mechanism of ATP production during autotrophic growth utilizing the Wood-Ljungdahl pathway

Much of the research and understanding of the Na^+ dependent acetogens results from research focused on *A. woodii* cell suspensions, which demonstrated that the Wood-Ljungdahl pathway in this organism was Na^+ dependent and established a sodium motive force across the cytoplasmic membrane (Heise et al., 1989). The electrochemical potential produced by this mechanism was determined to be more than -90 mV and was found to be more than sufficient to drive the conversion of ADP to ATP (Heise et al., 1989). Follow up studies further emphasized the necessity of the Na^+ gradient by demonstrating the inhibition of ATP synthesis through the addition of sodium ionophores to cell suspensions (Heise et al., 1989). The Na^+ motive force was created through a series of steps converting methylene- H_4F to methyl-CODH/ACS and CFeSP. To date direct evidence is lacking to determine which step in the three step

conversion is responsible for the pumping of Na^+ outside the cell. However, some skepticism remains as to whether the methylene- H_4F pathway is the sole mechanism responsible for Na^+ extrusion (Heise et al., 1989).

Biochemistry:

As mentioned previously, the Wood-Ljungdahl pathway begins with the reversible reduction of carbon dioxide to formate via the enzyme formate dehydrogenase (Ragsdale and Pierce, 2008). Formate dehydrogenases vary greatly among organisms, often utilizing one of several groups of electron acceptors and various prosthetic groups. However, most formate dehydrogenases use tungsten and selenium prosthetic groups and ferredoxin as electron acceptors to catalyze the reduction of carbon dioxide with NADH^+ (Ragsdale and Pierce, 2008). Following the reduction of carbon dioxide, formate is activated and bound to tetrahydrofolate (H_4F) producing formyl- H_4F via formyltetrahydrofolate synthetase (Ragsdale and Pierce, 2008). Next, a water molecule is removed from formyl- H_4F via formyltetrahydrofolate cyclohydrolase to yield Methenyl- H_4F (Ragsdale and Pierce, 2008). Methenyl- H_4F is then reduced via methylenetetrahydrofolate dehydrogenase to produce methylene- H_4F (Ragsdale and Pierce, 2008). Further reduction catalyzed by methylenetetrahydrofolate reductase converts Methylene H_4F into Methyl- H_4F . At this stage in the Wood-Ljungdahl pathway, the methyl group of Methyl- H_4F is transferred to a CFesP, a corrinoid iron sulfur protein containing a corrinoid cofactor and iron sulfur clusters, via the enzyme methyltransferase (Hu and Wood, 1984). Next, the methyl group is transferred to CO dehydrogenase / acetyl-CoA synthase (CODH/ACS), which condenses the methyl group with a molecule of CO produced from the oxidation of an additional molecule of CO_2 by CODH/ACS, to form acetyl-CoA (Meyer and Mörsdorf, 1993).

Finally, phosphotransacetylase converts acetyl-CoA to acetyl phosphate, followed by the production of acetate and the production of ATP via the conversion of Acetyl-P to acetate through the use of acetate kinase (Ragsdale and Pierce, 2008). As expected, the multiple reducing equivalents required to complete this process are generally provided by the oxidation of molecular hydrogen when grown autotrophically, via NADH and reduced ferredoxin during heterotrophic growth, and via direct or indirect

electron transfer when grown on a cathode with a sufficiently negative poised potential (Ragsdale and Pierce, 2008).

While many of the enzymes involved in the Wood-Ljungdahl pathway are found throughout the anaerobic biosphere, several enzymes of the pathway are quite unique to acetogens and will be reviewed here. One of the most important and unique enzymes in this pathway is CO dehydrogenase/ acetyl-CoA synthase (CODH/ACS). As discussed earlier, when acetogens are grown autotrophically, CODH/ACS catalyzes the condensation of a methyl group with a molecule of CO produced from the oxidation of an additional molecule of CO₂ (Meyer and Mörsdorf, 1993). Both of these processes are non-reactive without CODH/ACS; however, when catalyzed reactions rates of up to 40,000 s⁻¹ have been reported (Meyer and Mörsdorf, 1993). There are two distinct types of CODH used in the Wood-Ljungdahl pathway: the nickel CODH which serves a single function, and the CODH/ACS which serves two functions. The nickel-CODH catalyzes reaction four reducing carbon dioxide to carbon monoxide, while the CODH/ACS catalyzes the conversion of carbon monoxide into acetyl-CoA by coupling reactions 3 and 4 (reactions 3 and 4 respectively) (Meyer and Mörsdorf, 1993).



While both classes of these enzymes serve different functions, their structures are very similar. Both enzymes are homodimeric, both contain five metal clusters and both share a mushroom shaped morphology (Doukov et al., 2002). The mechanism by which CODH functions involves a back and forth style reaction whereas CODH is reduced by carbon monoxide in the initial step, followed by oxidation of the complex through the transfer of electrons to an external mediator like ferredoxin (Ragsdale, 2007). As mentioned earlier, the complex of ACS with CODH forms an enzyme with two distinct roles. The CODH portion of this complex converts carbon dioxide to a carbon monoxide intermediate at which point the ACS portion of the complex catalyzes the condensation of carbon monoxide, Co-A, and the methyl group of the methylated corrinoid iron-sulfur protein to generate acetyl-CoA (Menon and Ragsdale, 1996). The mechanism by which this occurs is currently the subject of much debate.

The second class of enzymes that are unique to the Wood-Ljungdahl pathway are the methyltransferase and corrinoid iron sulfur proteins. Methyltransferase proteins assist in transferring the methyl group from $\text{CH}_3\text{-H}_4$ folate to the cobalt site in the cobalamin cofactor bound to CFeSP (Hu and Wood, 1984). Methyltransferase is part of a group of B_{12} dependent family of enzymes (Hu and Wood, 1984). It was determined that $\text{CH}_3\text{-H}_4$ folate binds tightly to methyltransferase within a negatively charged portion of triose phosphate isomerase (Hu and Wood, 1984). A key process in this mechanism is the activation of an inactivated methyl group of methyltetrafolate since the activation requires the displacement of an amine bond which is stronger than the resulting $\text{CH}_3\text{-Co}$ bond that forms as a result (Hu and Wood, 1984). This displacement is believed to be possible due to a protonation process that helps to lower the activation energy needed for nucleophilic displacement of the methyl group by the Co(I) nucleophile (Hu and Wood, 1984).

Corrinoid iron sulfur proteins interact between $\text{CH}_3\text{-H}_4$ folate-methyltransfers and the CODH/ACS described in detail earlier. CFeSP has been characterized as an 88kDa heterodimeric protein which, as indicated by its name, contains an iron sulfur cluster as well as a cobalt cobamide cluster (Ragsdale et al., 1987). As expected, the Fe-S cluster plays an important role in interfacing between several subunits of ACS and methyltransfers in a three-step process. In the first step of this process, a methylation complex between the activated Co-I region of CFeSP binds to the methyltransferase in order to receive the methyl group from methyltetrahydrofolate in order to form methylated CFeSP, which is the second step of the process (Matthews, 2001). Thirdly, the newly methylated corrinoid iron sulfur complex forms a complex with ACS producing acetyl-CoA and yielding an inactive corrinoid complex which can be recycled (Matthews, 2001).

Acetogens represent a unique type of metabolism that is capable of assimilating CO_2 into multi-carbon compounds suitable for use as precursors for the production of biofuels. What makes acetogens even more unique is the ability of some members to interface with a graphite electrode in a manner that allows them obtain an essentially unending supply of reducing power. While literature has firmly established the ability of pure culture to carry out this process, mixed microbial consortia possibly represent

a more robust and industrially viable means of converting carbon dioxide into biofuel precursors or directly to biofuels.

CHAPTER TWO

MATERIALS AND METHODS

Environmental sampling:

Salt marsh sediment samples were collected from Edisto Island, South Carolina in March 2011. Samples were collected from the top 5 cm of the sediment associated with salt marsh cordgrass during low tide conditions and transported to the laboratory in covered 500 mL sterile vessels transported in an insulated container in light free conditions. Once in the laboratory, the samples were processed within 24 hours.

Keowee Lake Samples were collected from Lake Keowee in Six Mile, South Carolina (34.851733,-82.892444). Samples were collected from the top 10cm of lake sediment under one meter of water. The sediment surface was covered with leaf litter and tree detritus. Samples were collected with a sterilized trowel and placed into sterile 50 mL Falcon™ tubes. Samples were transported to the laboratory in an insulated light free container, and stored at 4 °C until processed. Samples were processed within 24 hours of their arrival to lab.

Clemson Experimental Forrest samples were collected from freshwater stream sediment fifty meters downstream of Waldrop Creek Falls (34.739629,-82.821808). Samples were collected from the top 10 cm of creek sediment under approximately 15 cm of water with a sterilized trowel and placed into sterile 50 mL Falcon™ tubes and transported to the laboratory in an insulated light free container, and stored at 4 °C until processed. Samples were processed within 24 hours of their arrival to lab.

Bovine rumen contents samples were collected from a fistulated dairy cow housed at the Clemson University LeMaster Dairy Farm (Clemson, SC). Rumen contents were extracted through a fistula and passed through sterile cheesecloth to removal large particulate matter. Rumen contents filtered in this manner were placed into a sterile 500 mL collection vessel. Collected samples were stored at 4 °C until processed. All samples were processed within 24 hours of collection.

Medium Composition and Growth conditions:

Acetogenic microbes were enriched using the following medium that contained per liter of deionized water: NaCl, 0.4g; NH₄Cl, 0.4g; MgCl₂, 0.33g; CaCl₂, 0.5g; KH₂PO₄, 0.5g; L-Cysteine HCl, 0.5g; and, NaHCO₃, 7.5g. The medium was amended with 10 mL of Wolfe's vitamin solution and 5mL of Wolfe's mineral solution. Wolfe's vitamin solution contained per liter of deionized water: Pyridoxine hydrochloride, 10mg; thiamine-HCL, 5.0mg; riboflavin, 5.0mg; nicotinic acid, 5.0mg; calcium D (+) pantothenate, 5.0mg; p-aminobenzoic acid, 5.0mg; thioctic acid, 5.0mg; biotin, 2.0mg; folic acid, 2.0mg; and, vitamin B12, 0.1mg. Wolfe's mineral solution contained per liter of deionized water: nitrilotriacetic acid, 1.5g; MgSO₄-7H₂O; MnSO₄-H₂O, 0.5g; NaCl, 1.0g; FeSO₄-7H₂O, 0.1g; CoCl₂-6H₂O, 0.1g; CaCl₂, 0.1g; ZnSO₄-7H₂O, 0.1g; CuSO₄-5H₂O, 0.01g; AlK(SO)₄-12H₂O, 0.01g; H₃BO₃, 0.01g; Na₂MoO₄-2H₂O, 0.01g. The final pH of the medium was adjusted to 6.8 ± 0.1 with 50% HCl under a headspace of high purity oxygen free H₂:CO₂ (80:20) gas and autoclaved at 121°C for 20 min.

Enrichments were initiated by aseptically introducing 5 mL sediment or rumen contents into degassed 120 mL sterile serum bottles containing 25 mL of enrichment medium under a headspace of H₂:CO₂ (80:20). Enrichments were incubated at 25 °C in static, light-free conditions. Subsequent enrichments received a 5% (vol/vol) inoculum from the previous generation in 20 mL serum bottles with 10 mL of the above medium and gas phase of high purity oxygen free H₂:CO₂ (80:20). Short chain organic acids and headspace gases were analyzed after seven days of incubation. Enrichments were continued for 13 generations or until a stable mixed microbial consortium was established based on acetate production with respect to time.

Growth curves of stable enrichment communities were performed in degassed in 20 mL serum tubes containing 10 mL of growth medium under a headspace of high purity oxygen free H₂:CO₂ (80:20). Optical density at 600 nm was measured using a spectrophotometer model Spec 20D (Thermo Scientific, Hampton, New Hampshire) calibrated with un-inoculated growth medium. Growth studies were carried out in triplicate.

Determinations of optimal growth conditions with regard to pH were examined by preparing growth medium as mentioned previously and manipulating the pH of the medium to 5.5 6.3 6.8 and 7.4 with 50% HCl or 5N NaOH.

Microbial Electrosynthesis Cell Design and Operation:

The microbial electrosynthesis cells (MEC) were constructed using 125 mL borosilicate glass serum bottles modified to operate in a two chamber “H cell” configuration (Chemglass Life Sciences, Wheaton, IL) as described by Marshall et al. (2012). Briefly, each chamber, cathode and anode, contained two 20 mm Balch-style ports capable of being sealed with butyl rubber stoppers and aluminum crimp caps, a 5 mm threaded o-ring sealed reference electrode port, and one 15 mm horizontal clamped o-ring junction designed to accept a Nafion membrane to separate both chambers, as shown in Figure 1. After assembly, Teflon tape was used to seal the horizontal and reference electrode ports on each chamber. The total volume of each chamber was 150 mL.

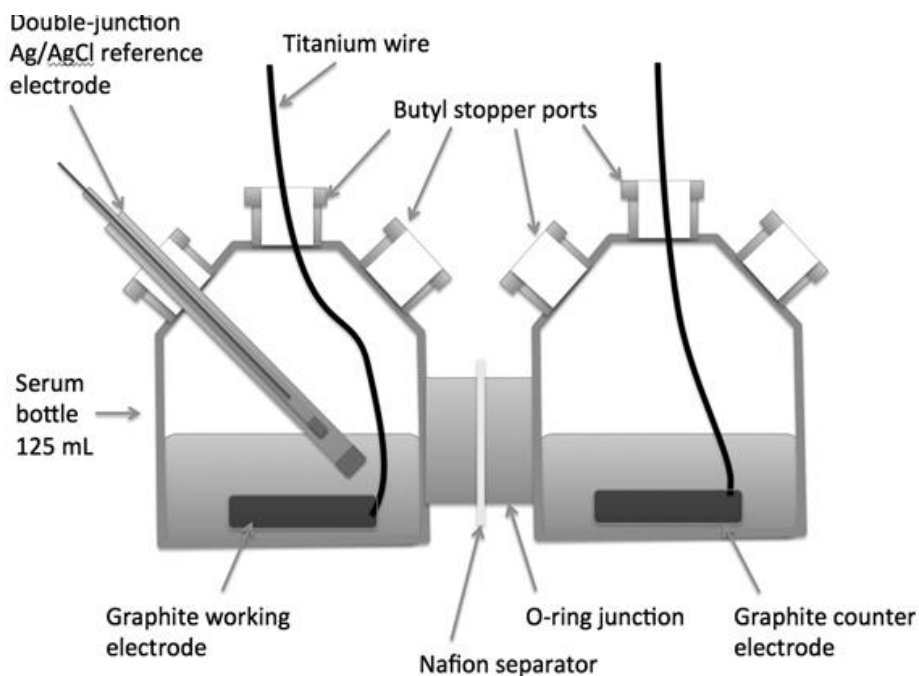


Figure 2.1: Microbial electrosynthesis cell design and construction. Each serum bottle has the capacity of approximately 150mL total volume, including headspace.

Double-junction reference electrodes were constructed in the laboratory and are described in the following information:

- Inner reference electrode junction: each electrode junction consisted of a Vycor® glass rod (BAS Inc. Tokyo, Japan) with a length of 2.85 mm, a diameter of 4.0 mm, a void volume of 28%, an average pore diameter of 40-200 Å, and an internal surface area of 250 m²/g was attached using PTFE heat-shrink tubing (BAS Inc. Tokyo, Japan) to a hollow glass rod with an inner diameter of 1.50 mm, an outer diameter of 3.00 mm, and a length of 132 mm.
- Outer reference electrode junction: these electrode junctions were constructed as described above except that the size of the glass tubing which was increased to an inner diameter of 4.00 mm and an outer diameter of 6.00 mm. The increased diameter allowed for insertion of the inner junction.
- Electroplating the silver wire: an 8 cm length of 99.9985% silver wire that was 0.5 mm in diameter (Alfa Aesar, Ward Hill, MA) was placed into a 500 mL beaker containing 3 M KCl, an extruded fine grain graphite electrode, and a previously prepared single junction Ag/AgCl (Inner junction filled with 3.5 M KCl) laboratory master reference electrode. A +0.1V potential measured against the Ag/AgCl laboratory master reference electrode was applied to the silver wire for 400 seconds using a model 1000B potentiostat (CH instruments, Austin, TX) to electroplate the silver wire with a layer of AgCl. Once plated the silver wire was inserted into the inner junction prepared previously and filled with 3M KCl.
- Double-junction reference electrode assembly: the inner reference electrode junction was inserted into an outer reference electrode junction, which was filled with growth medium prepared as above with the exception of withholding L-cysteine HCl. Parafilm was used to seal the interphase between the inner and outer junction to reduce evaporation.
- The potentials reported in this study have been converted to the Standard Hydrogen Electrode for the sake of simplicity by subtracting -210 mV from the potentials applied against AgCl.

The cathode and anode in each MEC chamber consisted of twenty five superfine grain high density extruded graphite rods measuring 30.0 mm x 6.35 mm (Graphite Store, Buffalo Grove IL). Before use, electrodes were cleaned by washing in acetone for 60 minutes, followed by boiling in deionized water for 120 minutes, and then drying overnight at 85 °C. The cleaned electrodes were then pretreated to remove metal contaminants by placing them into concentrated nitric acid at room temperature for 5 h followed by rinsing in deionized water until a neutral pH was reached. All electrodes used were conditioned in this manner. Electrodes were inserted into the cathode and anode chambers and placed in contact with a graphite electrode suspended with a titanium wire that served as a current collector. The titanium wire was inserted through a butyl rubber stopper. Cathode and anode chambers were separated by a cation exchange membrane (Nafion 117, Sigma Aldrich) pretreated by boiling in H₂O₂ (30% vol/vol) for 30 minutes, followed by soaking in 0.5M H₂SO₄, and deionized water for one hour each. An eight-channel potentiostat (model 1000B, CH Instruments, Inc., Austin, TX) was used for electrochemical control of the MECs.

Growth of the microbial consortium in the MECs was initiated by filling each of the chambers with 50 mL of growth medium, as described above but without L-cysteine HCL, in an anaerobic chamber (Coy Lab Products, Grass Lake, MI) with a N₂:H₂ (95:5) atmosphere. A 1% (vol/vol) inoculum from an eighth generation enrichment community was aseptically transferred into the cathode chamber, the headspace was flushed with H₂:CO₂ (80:20) for 10 minutes and the MECs were incubated in the anaerobic chamber at 25 °C at a potential of -790 mV.

Approximately every three days samples were taken from the cathode chamber for short chain volatile fatty acid and headspace analyses. On the seventh day of operation in this manner, the cathode and anode supernatants were removed and replaced with 50 mL of sterile medium. The headspace was then flushed with N₂:CO₂ (80:20) for 10 minutes. Cathodic biofilm and small volumes of supernatant that were unable to be removed served as the source of inoculum for subsequent generations. Again, a potential of -790 mV was applied. Subsequent medium exchanges and cathode sampling occurred in this same manner under a N₂:CO₂ (80:20) headspace. Cathode pH was measured in conjunction with cathode supernatant

sampling. If a pH was measured above 7.5, the cathode compartment was sparged with N₂:CO₂ (80:20) for 10 minutes until pH was restored to 6.8.

Analysis of acetate production using ¹³C bicarbonate was conducted using two replicates of the previously described acetogenic MEC systems that were established by a placing a 1% (vol/vol) inoculum from an existing MEC into the cathode chamber of each replicate and each headspace was flushed with H₂:CO₂ (4:1) for 10 minutes. A potential of -790 mV was applied. Following 7 days of incubation at 25 °C, the supernatant was removed and replaced with fresh medium under a N₂:CO₂ (80:20) headspace, followed by sparging with N₂:CO₂ (80:20) for 10 minutes, and a potential of -790 mV was applied. After an additional seven days of incubation the two replicates were assessed for acetate production to assess parity between the replicates. The labeling study began with a third medium exchange performed as described previously with the following exceptions: 1) the control cell received 50 mL of growth medium as described previously under a N₂ headspace without sparging to prevent loss of bicarbonate; 2) the experimental cell received growth medium having 10 mol % ¹³C bicarbonate under a N₂ atmosphere and promptly sealed with a butyl rubber stopper. The potential was reapplied. Following four days of incubation, supernatant samples were removed for analysis.

A separate evaluation was conducted to evaluate the requirement for potential to be present for the microbial production of acetate. Two replicates of the previously described acetogenic MEC systems were established by a placing a 1% (vol/vol) inoculum from an existing MEC into the cathode chamber of each replicate followed by flushing with H₂:CO₂ (80:20) for 10 min. A potential of -790 mV was applied. After 7 days incubation at 25 °C, the supernatant was removed from the cathodic chamber and replaced with fresh sterile medium under a N₂:CO₂ (80:20) headspace and sparged with N₂:CO₂ (80:20) for 10 min. Following an additional seven days of incubation as before the supernatant was removed from the cathodic chamber and replaced with fresh sterile medium under a N₂:CO₂ (80:20) headspace and sparged with N₂:CO₂ (80:20) for 10 min and a potential of -790 mV was reapplied. Following the second medium exchange, subsamples were removed from the cathodic chamber and the acetate concentration was measured as described above. Acetate production rates and current consumption were monitored during a three-day period at which time the applied potential of -790 mV was removed. The MEC was operated as

an open circuit, without potential, for 36 hours during which time the MEC supernatant was monitored for acetate production. A potential of -790 mV was then re-applied to the cathode and the supernatant was again measured for acetate production and current consumption.

Cyclic voltammetry (CV) was performed using the above MEC system. CV was conducted with a scan rate of 0.002 V sec^{-1} from an initial applied potential of 0 V to a low potential of -0.6 V , three sweep segments were carried out following an initial quiet time of 5 seconds. Sensitivity of the scan was set at 0.001 A V^{-1} . Baseline CV scans were obtained from abiotic MEC. Experimental CV scans were taken from an acetogenic MEC producing more than $3.0 \text{ mM acetate L}^{-1} \text{ day}^{-1}$ in the following configurations, supernatant in the cathode compartment was completely removed from the functioning MEC and replaced with sterile growth medium, cathode supernatant from the functioning MEC was passed through a $0.2 \text{ }\mu\text{M}$ sterile filter then placed in the cathode compartment containing sterile electrodes, and finally, an biotic MEC system was scanned with the above parameters.

Consortium Analysis:

Denaturing gradient gel electrophoresis (DGGE) analysis was performed to evaluate subsets of the parent electroacetogenic cow rumen consortium. Total DNA was extracted from 4.0 mL of supernatant from the cathode chamber using the UltraClean Microbial DNA Isolation Kit by following the manufactures protocols (MO BIO Laboratories Inc., Carlsbad, CA). 16S rDNA was amplified using primers targeting the V3 region of the 16S bacterial rDNA gene. PCR reactions of 50 μ L total volume were set up as follows: 25 μ L Master Mix (Promega, Fitchburg, Wisconsin), 1.25 μ L of 10 μ M forward primer - PRBA 338F: 5'-ACTCCTACGGGAGGCAGCAG-3' (Integrated DNA Technologies, Coralville, Iowa), 1.25 μ L of 10 μ M reverse primer - PRUN 518R: 5'-ATTACCGCGGCTGCTGG-3' (Integrated DNA Technologies, Coralville, Iowa), and 17.5 μ L of DNase free water (Farnleitner et al., 200).

Additionally, each primer was amended with a high GC content sequence - 5'-

CGCCCCCGCGCGCGGGCGGGGCGGGGGCACGGGGGG-3' attached to the 5' end of the forward primer rendering it suitable for DGGE analysis. PCR amplification was performed in an Ep Mastercycle (Eppendorf, Hamburg, Germany) with the following protocol: initial denaturation temperature

of 94°C for 9 minutes, 30 PCR cycles were followed by a terminal extension period of 7 minutes at 72°C; denaturation, annealing, and elongation were set at 94° C, 55° C, and 72° C for 30 seconds each. All PCR products were checked for amplification of appropriate length using agarose gel electrophoresis. PCR purification was performed using the Qiagen QIAquick PCR Purification Kit (Qiagen, Valencia, CA) by following the manufacturer's protocol.

Community subsets of the electroacetogenic cow rumen consortia were created through serial dilutions in sterile anaerobic water. Dilutions were created from dilution factors of 10^{-1} through 10^{-6} . These dilutions were then transferred to enrichment growth conditions described above. Subsequent acetate production for each of the consortia subsets was quantified. Based on acetate production rates, consortia subsets were chosen for evaluation in MEC systems as described previously.

DGGE analysis was performed on consortia subsets using a D-CODE denaturing gel electrophoresis system according to the manufacturer's instructions (Bio Rad, Inc. Vienna, Austria). Briefly, an 8% polyacrylamide gel with a parallel poured denaturing gradient ranging between 30% and 50% held at 60°C at 90V for 16 hours in 1X tris-acetate-EDTA buffer. Gels were visualized and photographed following 15 minutes of staining in 750µL of 1X TAE buffer to which 75µL Sybr Gold (Invitrogen, Carlsbad, California) was added. Developed gels were visualized with UV transillumination using a Gel-Doc (BioRad, Vienna, Austria).

16S rRNA sequencing was carried out according to Marshall et al., (2012) and Fichot and Norman (2013). Briefly, samples for rRNA extraction were collected in TRIzol (Invitrogen, Carlsbad, California) by filtration through a 0.22 µm Sterivex filter (Millipore, Billerica, Massachusetts) and stored at -80 °C until processed. Reverse transcription was carried out using random hexamers and PCR was performed targeting the V1-V3 region using universal bacterial primers. PCR products were cleaned up using a commercial clean up kit (Qiagen, Venlo, Netherlands). Amplicons were sequenced using the Pacific Biosciences RS sequencer (Engencore, LLC Columbia, South Carolina).

Analytical Methods:

Subsamples from the cathode were aseptically removed for short chain volatile acid and alcohol analyses. A 450 μ L aqueous sample was loaded on a gas chromatograph (Agilent 7890A) equipped with a DB-FFAP column (Agilent J&W, 25m, 0.32mm, 0.5 μ m) as follows: 1 μ L of sample was injected into the gas chromatograph by auto-sampler (Agilent 7683b). Inlet pressure was maintained at 16.2 psi with a total flow of 52.5 mL/min, and an injector temperature of 230 °C. Flow through the column was 0.64 mL/min. Initial oven temperature was 60 °C. After holding for one minute, oven temperature was increased to 120 °C at a rate of 3 °C/min, then increased to 160 °C at a rate of 65 °C/min, and finally increased to 220 °C at 15 °C/min where it was held for 2 min. The ultra-high purity hydrogen flow rate was set to 30 mL/min. The scientific grade air flow rate was 400 mL/min. The makeup gas, ultra high purity helium, flow rate was 25 mL/min.

The composition of headspace gases was assessed by collecting 0.5mL of headspace with a 1.0 mL tuberculin syringe (VWR, Randnor, PA). Collected headspace was injected into a gas chromatograph (Agilent 7890A) equipped with a HP-PLOT Molesieve column (30m x 0.32mm x 3 μ m). GC parameters were as follows: inlet temperature was maintained at 250 °C, a split ratio 10:1 and 8.63 psi. Total flow rate was 102 mL/min. Initial oven temperature was held at 50 °C for 90 seconds then increased to 150 °C at a rate of 50 °C/minute at which point the temperature was held stable for 2 minutes. The detector was a thermal conductivity detector (TCD) held at 250 °C with a reference (UHP Helium) flow of 20mL/min and a makeup flow of 2 mL/min set at a constant pressure of 8.87psi.

To volatilize the ¹³C-labeled acetate and render it suitable for GC-MS analysis, butyl esters were prepared by removing one mL of cathode supernatant from the duplicate MECs, which was filtered through a 0.2 μ M PTFE filter and added to 20 mL screw-cap tubes containing 2 mL of a solution containing 20 mL n-butanol, 5 mL H₂SO₄ solution and 0.8mL of hexane. After vortexing for 5 min, the tubes were heated to 80 °C for 2 hours then cooled to room temperature. The hexane phase was removed and stored at 4 °C until analyzed using an Agilent 7890A gas chromatograph equipped with a 5976C inert Mass Selective Detector (MSD). One μ L of sample was injected into the GC-MS by auto-sampler (Agilent 7683b). The inlet was held at 250 °C with 6.45 psi of carrier gas, UHP helium. The initial oven temperature was set to 30 °C that

was held for one minute and then increased at a rate of 5 °C per minute for 6 minutes. The column was a J&W Scientific DB5-ms (30m x 0.25mm x .025µM). Carrier gas flow rate through the column was 1mL/min. The MSD was operated to scan in the 30-120 m/z range.

Electrode samples for Scanning Electron Microscopy (SEM) were collected from acetogenic MEC cells producing ~3.0mM acetate day⁻¹. The electrode samples were transferred to 3.5 % glutaraldehyde in 0.1 M cacodylate buffer (pH 7.0). After fixation, electrodes were dehydrated using a series of incubations with increasing percentages of ethanol ranging from 75 to 100 %. Finally, the electrode samples were treated with hexamethyldisilazane and allowed to air dry. After drying, the samples were gently adhered horizontally to aluminum specimen support stubs using double-sided carbon tape. The samples were then imaged using a Hitachi S-6600 scanning electron microscope under a vacuum of 30 Pa.

CHAPTER THREE

RESULTS

The assessment of various environments for acetogenic consortia resulted in six mixed microbial consortia being obtained from two freshwater lake sediment samples, two salt marsh sediment samples, and one freshwater river sediment sample. While several early enrichment generations produced detectable levels of methane production, subsequent generations lost methanogenic capability. Enrichments showed increasing acetate production beginning after the second generation and were continued until a stable acetogenic community was obtained. Stability was evaluated based on total acetate production during subsequent seven-day periods of incubation generations at a temperature of ~20 °C as shown in **Table 3.1**, **Figure 3.1** and **Figure 3.2**. Enrichment communities had obtained stability by the eight generation and enrichments were continued for as long as thirteen generations.

Enrichment Source	Enrichment Generations	Initially Methanogenic	Methanogenesis Eliminated	Stable Community
Freshwater Sediment	8	No	Yes	Yes
Salt Marsh Sediment	8	Yes	Yes	Yes
Bovine Rumen Fluid	8	Yes	Yes	Yes
Freshwater Forrest River Sediment	8	No	Yes	Yes

Table 3.1: Sources and results of acetogenic enrichment from several different environments

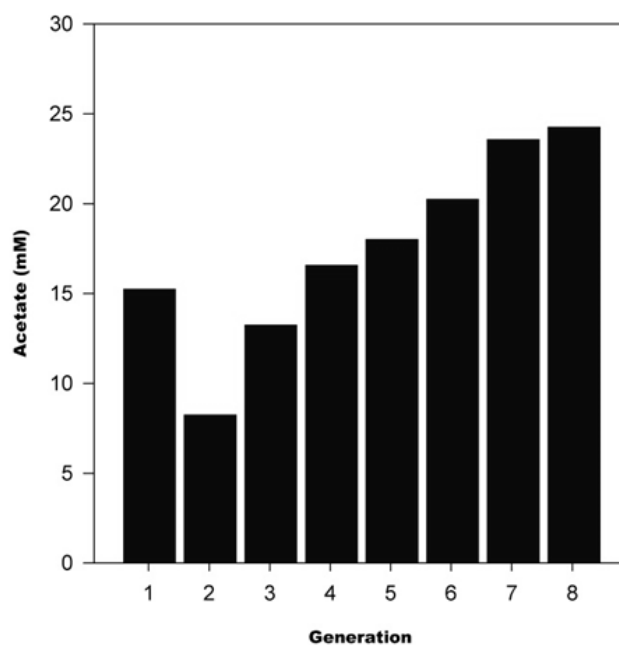


Figure 3.1: Acetate production per enrichment generation of Salt Marsh 1 consortium grown in enrichment conditions on H_2 and CO_2 . Acetate production shown following seven days of incubation at room temperature in light free conditions for a salt marsh sediment inoculum one.

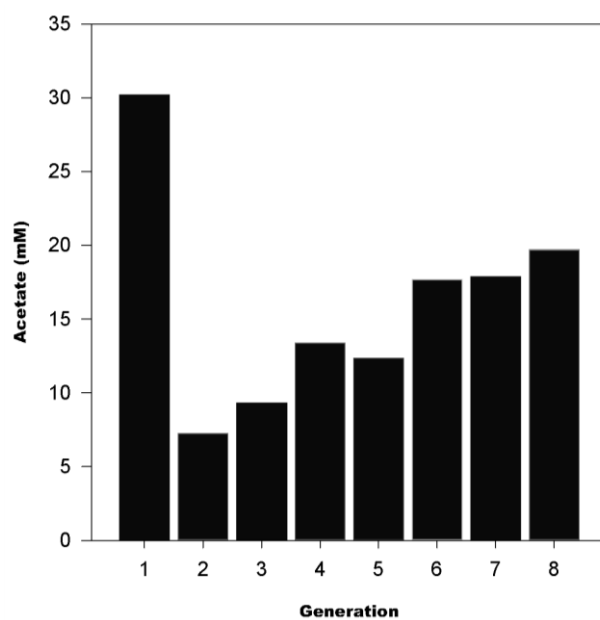


Figure 3.2: Acetate production per enrichment generation of Cow Rumen 1 consortium grown in enrichment conditions on H_2 and CO_2 . Acetate production shown following seven days of incubation at room temperature in light free conditions for a cow rumen inoculum one.

Stable enrichment communities were introduced into MEC systems (described previously) and evaluated for electrosynthetic production of acetate. Of the six enrichment communities screened, only two were found to produce acetate through the consumption of carbon dioxide and electrical current provided via a cathode poised at reductive potential. The salt marsh sediment 1, and bovine rumen fluid consortium. Those communities that failed to consume current after 30 days of incubation were determined not to be capable of electrosynthetic production of acetate under the growth conditions used in this study.

A MEC inoculated from salt marsh sediment culture was operated for over 54 days at a fixed cathode potential of -590 mV. Acetate production from the MEC prior to the second medium exchange (Day 14) is omitted to reduce concerns that acetate production may have occurred from stored energy or products while the culture was initially grown under a hydrogen / carbon dioxide headspace for the first seven days. Following the second exchange of supernatant (Day 14), electrosynthetic acetate production was detected as the sole observable end product. Acetate production rates were as high as 0.05 mM day^{-1} (**Figure. 3.3**). Using the estimated cathode surface area of 9.55 cm^2 a peak acetate production rate of $5.24 \text{ } \mu\text{M acetate day}^{-1} \text{ cm}^{-2}$ was calculated. Total accumulation of acetate was 3.21 mM during the 54 day incubation period and resulted from the consumption of 1301 C by the microbial consortium. Electrons recovered as acetate after 54 days were calculated to be 198 C, representing a total Coulombic efficiency of 15.24% (**Figure 3.4**). The cathode chamber pH ranged between 6.8 and 8.0 during the experiment (**Figure 3.5**).

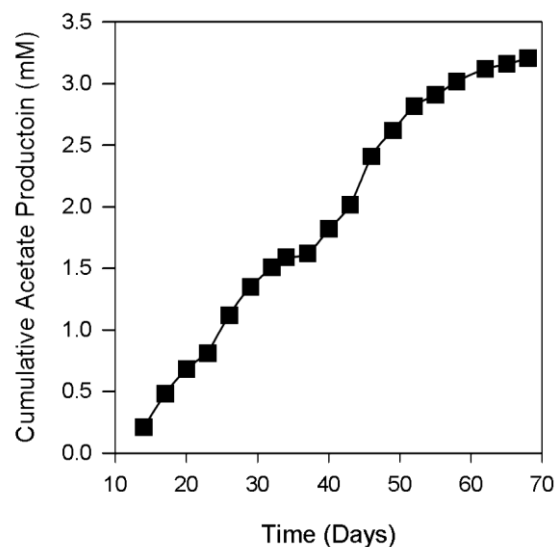


Figure. 3.3 Cumulative electrochemical acetate production of Salt Marsh 1 consortium grown at -590 mV. Cumulative acetate concentration (■) in an MEC containing a salt marsh-derived microbial consortium.

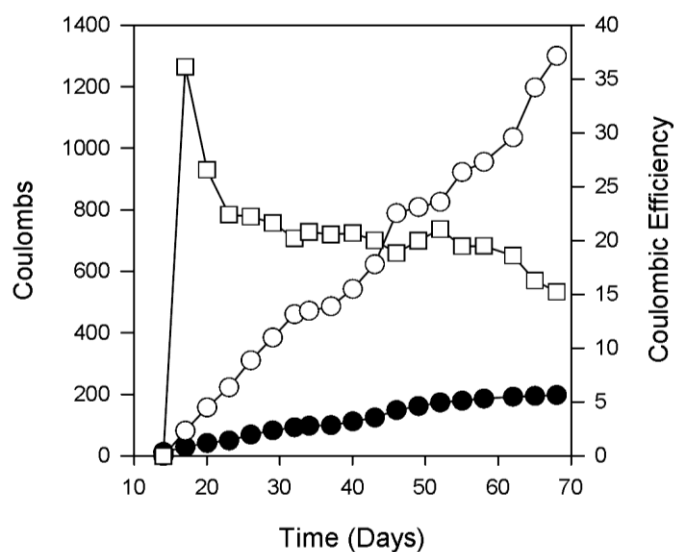


Figure. 3.4 Cumulative current consumption and coulombic efficiency of Salt Marsh 1 grown at -590 mV. Coulombs consumed by the MEC (○). Calculated coulombs recovered in acetate (●). Coulombic efficiency (□) calculated with respect to acetate production.

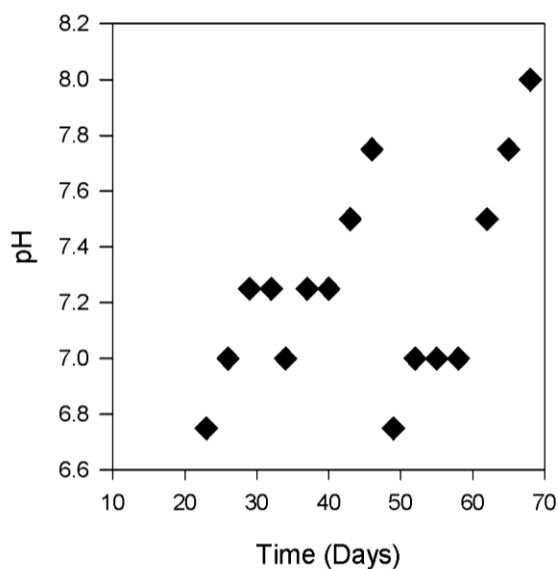


Figure. 3.5 Measured cathode compartment pH of Salt Marsh 1 grown at -590 mV. Measured pH (♦) of cathode compartment.

A MEC inoculated from cow rumen enrichment culture was operated for over 45 days at a fixed cathode potential of -790 mV. Acetate production from the MEC prior to the second medium exchange (Day 14) is omitted to reduce concerns that acetate production may have occurred from stored energy or products while the culture was initially grown under a hydrogen headspace for the first seven days. Following the second exchange of supernatant (Day 14), electrosynthetic acetate production was detected as the sole observable end product. Acetate production rates were as high as 3.3 mM day^{-1} (**Figure. 3.6**). Using the estimated cathode surface area of 165 cm^2 a peak acetate production rate of $0.054 \text{ mM acetate day}^{-1} \text{ cm}^{-2}$ was calculated. Total accumulation of acetate was 50.3 mM during the 30 day incubation period and resulted from the consumption of 2233 C by the microbial consortium. Electrons recovered as acetate after 30 days were calculated to be 1746 C , representing a total Coulombic efficiency of 78.2% (**Figure 3.7**).

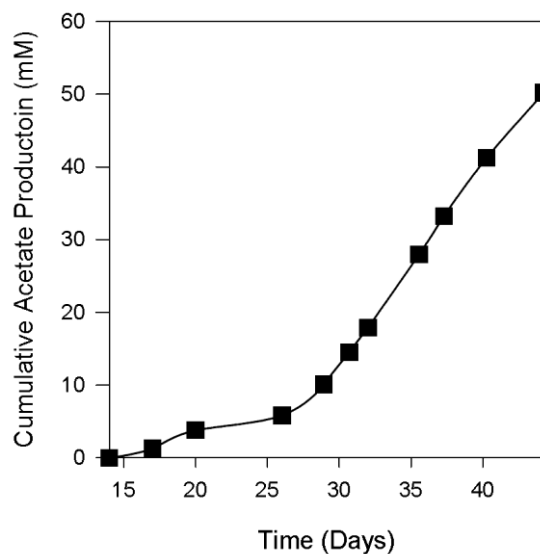


Figure. 3.6 Cumulative electrochemical acetate production of Cow Rumen 1 consortium grown at -790 mV. Acetate concentration (■) in an MEC containing a cow-rumen-derived microbial consortium.

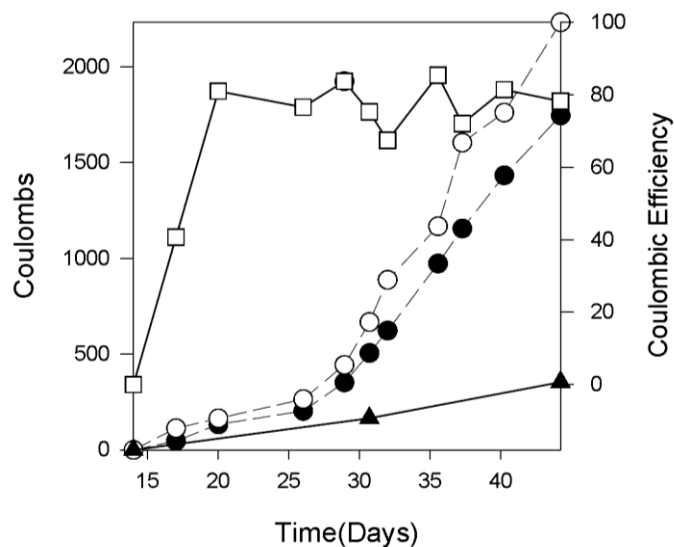


Figure. 3.7 Cumulative current consumption and coulombic efficiency of Cow Rumen 1 grown at -790 mV. Coulombs consumed by the MEC (○). Calculated coulombs recovered in acetate (●). Coulombic efficiency (□) calculated with respect to acetate production. Coulombs consumed in an abiotic control MEC (▲); acetate was not produced in the abiotic control MEC.

Figure 3.8 shows that the pH of the cathode compartment varied between 6.5 and 8.5 during the 30-day incubation period. Beginning at day 29, pH readings above 7.0 were observed and modified by sparging the cathode headspace with N₂:CO₂ (4:1) for ten minutes until the pH was below 7.0. As shown in **Figure 3.8**, the pH was controlled in this manner three times. Following day 32 pH control was not needed.

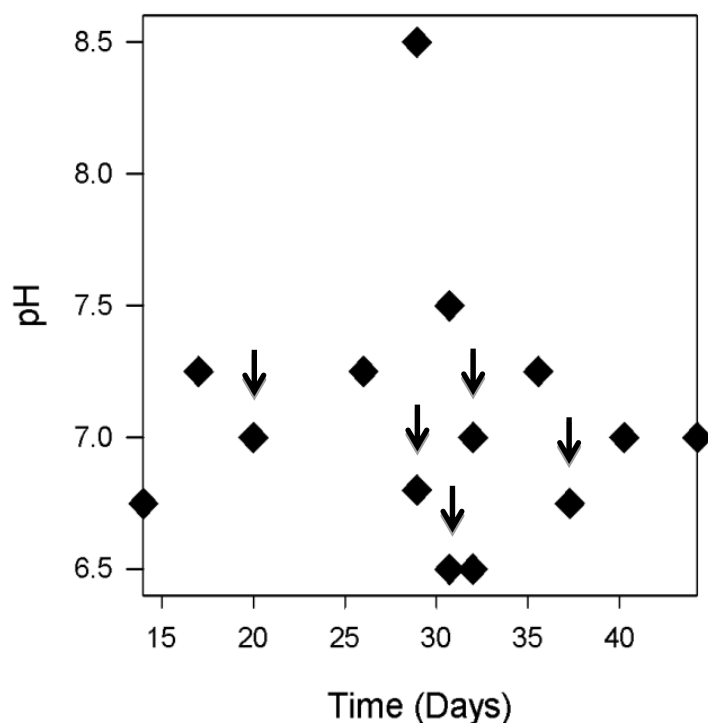


Figure. 3.8 Measured cathode compartment pH of Cow Rumen 1 grown at -790 mV. Measured pH (♦) of cathode chamber. Arrows indicate a medium exchange or headspace flushed with N₂:CO₂ (4:1) to control pH.

The MECs operating in a three-electrode configuration poised at sufficiently low cathode potentials had the possibility for abiotic electrochemical hydrogen production in accordance with the equation $2\text{H}_2\text{O} + 2\text{e}^- \rightarrow \text{H}_2 + 2\text{OH}^-$. Because abiotic hydrogen represents a source of reducing power for the microbial production of acetate from CO₂ it was necessary to evaluate whether hydrogen was being produced under the conditions used and, if so, to quantify its rate of production. By doing so, it will be

possible to distinguish between acetate evolved from abiotic hydrogen production and acetate produced via electrosynthesis. The MEC configuration was evaluated for abiotic hydrogen production at a cathode poised potential of -790 mV vs. SHE. Abiotic hydrogen production was detected at an average rate of $0.045 \text{ mmol day}^{-1}$ which over nine days produced approximately 0.4 millimoles of hydrogen (**Figure 3.9**). Electron recovery in the abiotic system varied between 80.3 – 90.2% with respect to electrons recovered as hydrogen (**Figure 3.10**). Theoretical acetate production resulting from this abiotic hydrogen can be calculated using the equation $4\text{H}_2 + 2\text{CO}_2 \rightarrow \text{CH}_3\text{COOH} + 2\text{H}_2\text{O}$ (one equivalent of acetate from four equivalents of hydrogen) and adjusting the yield for a reaction liquid volume of 50 mL. Based on this information, the maximum rate of acetate production that may result from the abiotic hydrogen production was estimated to be $0.23 \text{ mM L}^{-1} \text{ day}^{-1}$ which is significantly less than the rate of $3.3 \text{ mmol L}^{-1} \text{ day}^{-1}$ observed for the actively growing microbial consortium (**Figure. 3.6**). Thus, abiotic hydrogen production could be less than a 10% contribution to acetate production by the microbial consortium enriched from the bovine rumen, but that contribution will be relatively small.

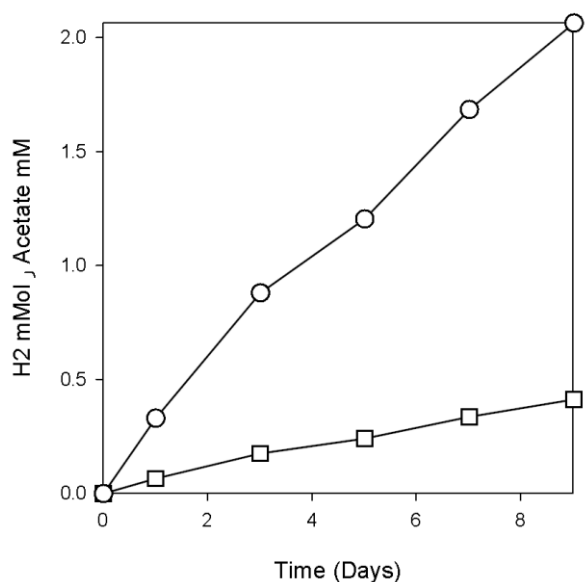


Figure 3.9: Quantification of abiotic hydrogen production rates for MEC systems operated at -790 mV. Cumulative hydrogen production (□) (mmol). Calculated theoretical acetate production (○) that could possibly result from abiotic hydrogen production.

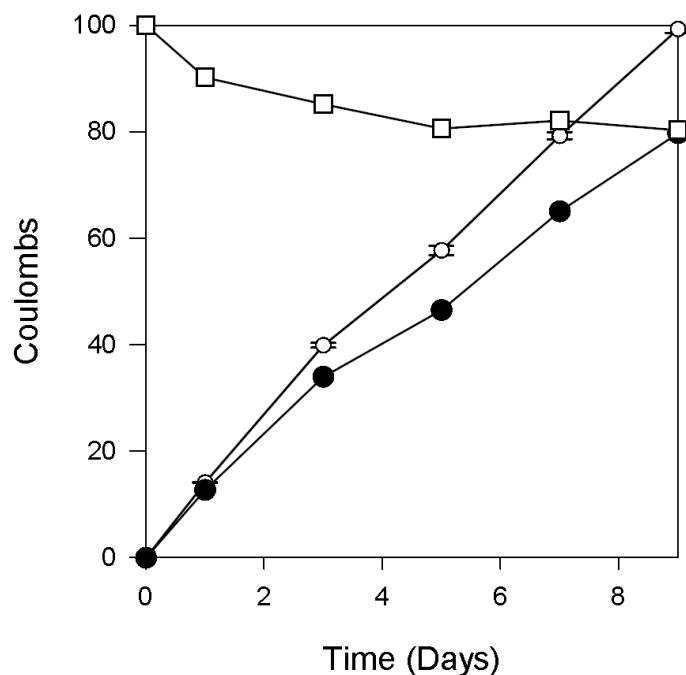


Figure. 3.10 Cumulative current consumption and coulombic efficiency for abiotic hydrogen production in a MEC system operated at -790 mV. Open circle (○) indicated total coulombs consumed by the MEC. Filled circles (●) indicate calculated coulombs recovered as hydrogen. Open square (□) indicates calculated coulombic efficiency in respect to hydrogen production.

The effect that different pHs of the growth medium might have on the production of acetate in the enrichment conditions is shown in **figure 3.11** utilizing a cow rumen inoculum removed from a functioning MEC system. Growth medium was prepared at pHs of : 5.5, 6.3, 6.8, and 7.4, representing carbon in the forms of carbon dioxide and bicarbonate in ratios ranging from 95:5 to 5:95. As shown in **figure 3.11**, the highest average acetate production occurred at a pH of 7.4 while the lowest average acetate production was observed at pH 5.5. A one way analysis of variance found that pHs of 7.4 and 6.8 were statistically different from that of 5.5 ($\alpha = 0.050$). A statistically relevant difference of acetate production was not found between the pH treatments at of 6.8, 7.4, and 6.3 treatments.

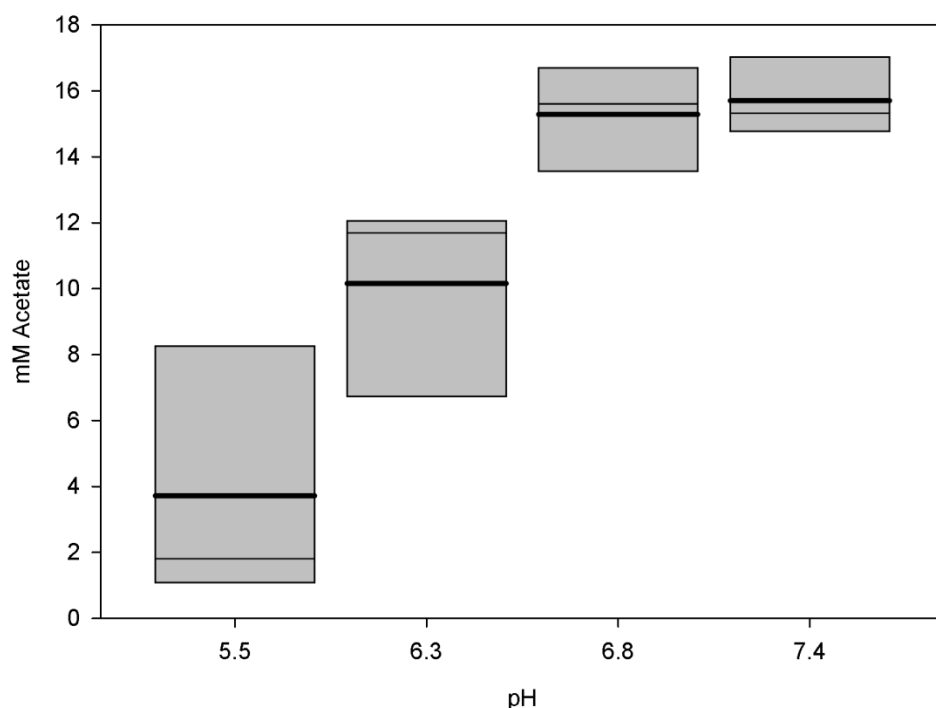


Figure 3.11: Evaluation of acetate production of Cow Rumen 1 consortium grown in enrichment conditions at varying pH levels. Black line indicated average acetate production, grey line represents median. The data range is indicated by the upper and lower bounds of the plot.

To evaluate whether the acetate produced by microbial electrosynthetic cells is derived solely from electrosynthetic CO_2 consumption, ^{13}C -labeled bicarbonate was added to the growth medium as described in the materials and methods. Cathode supernatant was removed and isotopic ratios for acetate were measured by GC-MS. Isotope ratio analysis is performed using the CH_3CO^+ fragment ion, which is formed following scission of the C-O bond for the butoxy derivatizing agent that was used to facilitate volatilization and GC separation. **Table 3.1** provides expected and measured peak intensities for ion fragments having mass-to-charge (m/z) ratios of 43, 44, and 45 that correspond to the possible fragments $^{12}\text{CH}_3^{12}\text{CO}^+$, $^{13}\text{CH}_3^{12}\text{CO}^+$ or $^{12}\text{CH}_3^{13}\text{CO}^+$, and $^{13}\text{CH}_3^{13}\text{CO}^+$. Results are presented for a control MEC in which ^{13}C labeled bicarbonate was not added, and for a MEC in which the bicarbonate in the medium had modified with the addition of 10 mole percent of ^{13}C -labeled bicarbonate, yielding a net bicarbonate ^{13}C abundance of 11 mole percent for that cell.

Expected peak intensities for the 43, 44 and 45 m/z ions were calculated using the natural ^{13}C abundance of 1.1 mole percent for carbonate in the control MEC, and the artificially high ^{13}C abundance of

11 mole percent for the experimental MEC. Fractionation of ^{12}C and ^{13}C during acetate formation was assumed not to occur, and isotopic distributions for H and O were not considered as these atoms have natural abundances near 100% in their most prevalent isotopic forms. MEC systems operated with the addition of ^{13}C -labeled bicarbonate yielded acetate that produced a peak intensity at $m/z=44$ that is approximately 22.9 percent of the peak intensity at $m/z=43$, in good agreement with the intensity of 24.7% expected from a simple probability calculation for the ^{13}C labeled bicarbonate sample but very different from the intensity of 2.2% expected for the non ^{13}C -labeled bicarbonate sample. The control experiment using a MEC without ^{13}C labeled bicarbonate produced acetate for which the intensity of the $m/z=44$ peak is 2.7% of that for the $m/z=43$ peak, in relatively good agreement with the expected intensity ratio from probability calculations. The agreement between measured and expected peak intensities at $m/z=44$ for the control sample and also for the $m/z=45$ peaks for both samples was not as good as it might have been because the peaks at $m/z=44$ and 45 are relatively small and the GC-MS used for this work is not intended for very precise isotope ratio analysis. Even so, the data are more than sufficient to state that acetate produced by these MEC systems comes from bioelectrosynthetic fixation of CO_2 /bicarbonate in the growth medium and not from a reservoir of stored carbon in the cells that might have carried over from previous enrichment cycles.

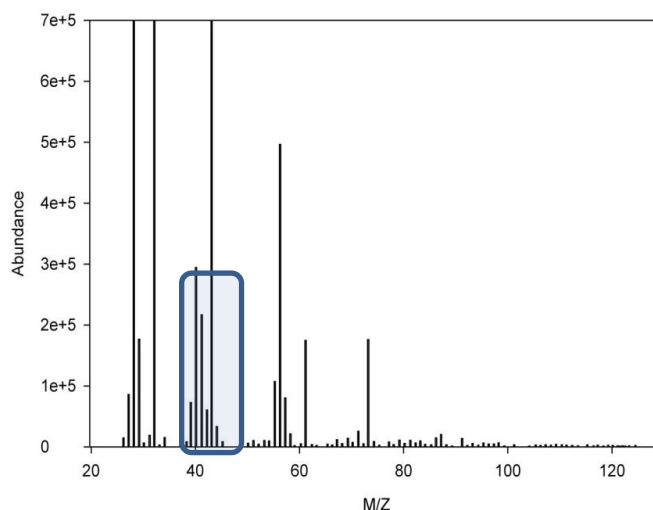


Figure 3.12: Mass spectrum profile of electrosynthetic acetate production of Cow Rumens 1 consortium grown on un-supplemented bicarbonate growth medium.

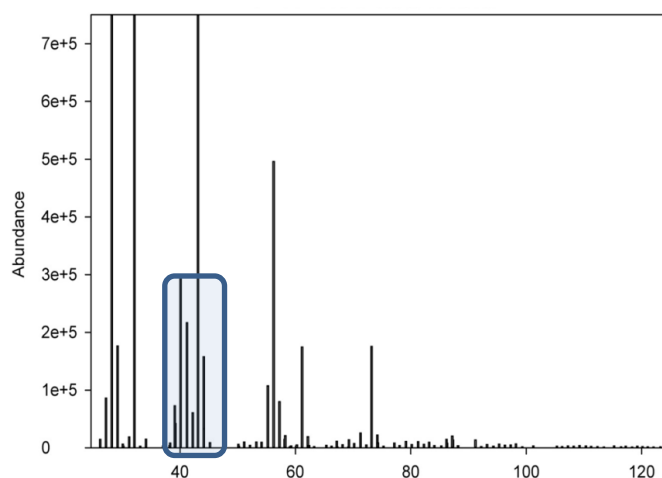


Figure 3.13: Mass spectrum profile of electrosynthetic acetate production of Cow Rumen 1 consortium growth on carbonate supplemented with 10 Mol percent ^{13}C

	Ion Structure	Expected Peak Intensity (Enriched)	Measured Peak Intensity (Enriched)	Expected Peak Intensity (Control)	Measured Peak Intensity (Control)
M/Z 43	$\begin{matrix} ^{12}\text{CH}_3 & ^{12}\text{CO}^+ \end{matrix}$	100%	100%	100%	100%
M/Z 44	$\begin{matrix} ^{13}\text{CH}_3 & ^{12}\text{CO}^+ \\ \text{or} \\ ^{12}\text{CH}_3 & ^{13}\text{CO}^+ \end{matrix}$	24.7%	22.9%	2.2%	2.7%
M/Z 45	$\begin{matrix} ^{13}\text{CH}_3 & ^{13}\text{CO}^+ \end{matrix}$	1.5%	1.13%	0.01%	0.78%

Table 3.2: Predicted and measured peak intensity of acetate fragments produced from a control MEC without ^{13}C labeled bicarbonate and the experimental MEC with growth medium supplemented with.

Cyclic voltammetry was performed on the MEC system to evaluate the presence of redox active molecules associated with the biotic cathodes. Redox peaks were not present in the abiotic control cathode in the range of 0 to -600 mV as indicated in **figure 3.14**. However, a large amount of capacitive double layer charging was observed and estimated to be $760 \mu\text{F} (\text{cm}^2)^{-1}$. In contrast, **figure 3.15** shows the same scan from 0 to -600 mV at 2mV/s for a biotic acetogenic cathode. The onset of catalytic current of the

biotic cathode started at $\sim -250\text{mV}$ vs. SHE with increased current remaining until the lower scan limit of -600 mV , however, there are two distinct catalytic waves present in that range. Unfortunately, due to the smaller peak height, midpoint potentials determined by first order integrals are uninformative. The large difference between the peak current in the abiotic scan and the biotic scan however are of note. A CV scan of spent cell free supernatant did not show any increased catalytic current when compared to the abiotic system.

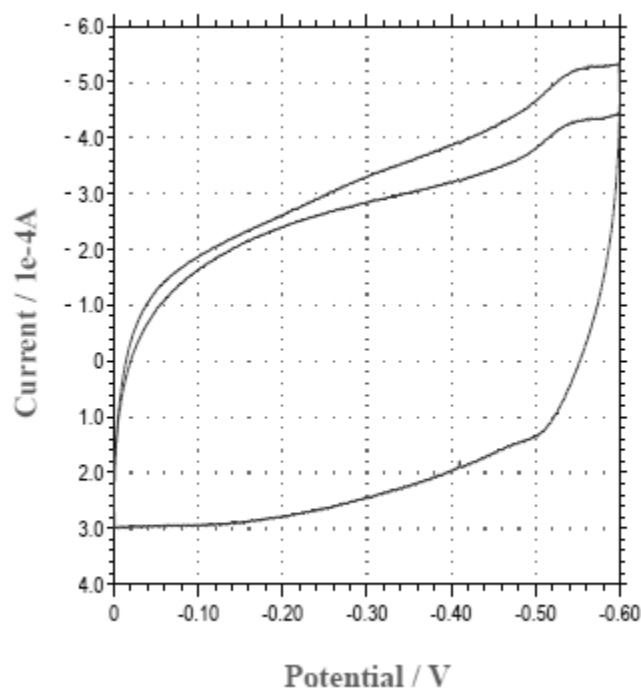


Figure 3.14 : Cyclic voltammetry scan of an abiotic MEC cathode immersed in sterile growth medium

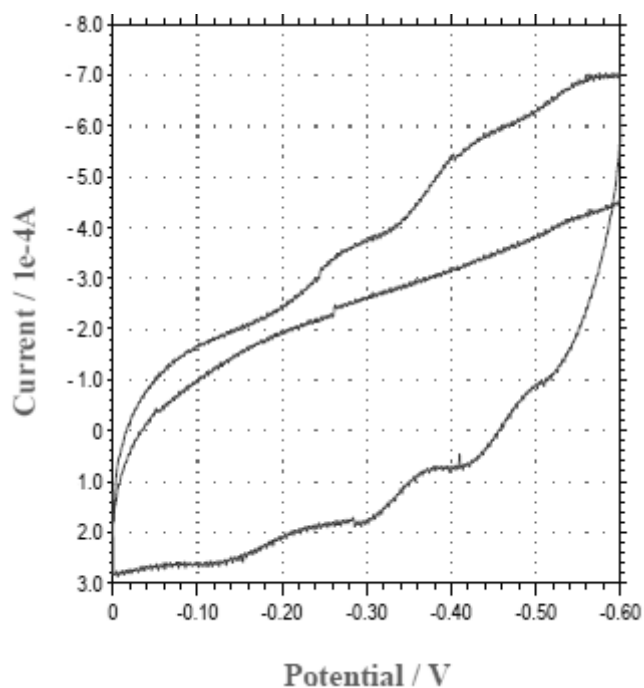


Figure 3.15: Cyclic voltammetry scan of a MEC cathode colonized by the electroacetogenic Cow Rumen 1 consortium immersed in sterile growth medium

Scanning electron microscopy was utilized to evaluate the presence and abundance of microbes growing in contact with the MEC cathode. As shown in **figure 3.16**, the observed bacteria were predominantly long thin rods varying in size from 2 to 2.5 μM growing in an EPS matrix. **figure 3.17** shows an area of a cathode colonized by short thick rods about 1 μM in length. Of the cathode area examined, bacterial presence was not uniform nor was the surface completely covered. A cathode electrode removed from an abiotic control was also examined using SEM. The abiotic electrode (**figure 3.18**) was absent of microbes or signs of EPS matrix.

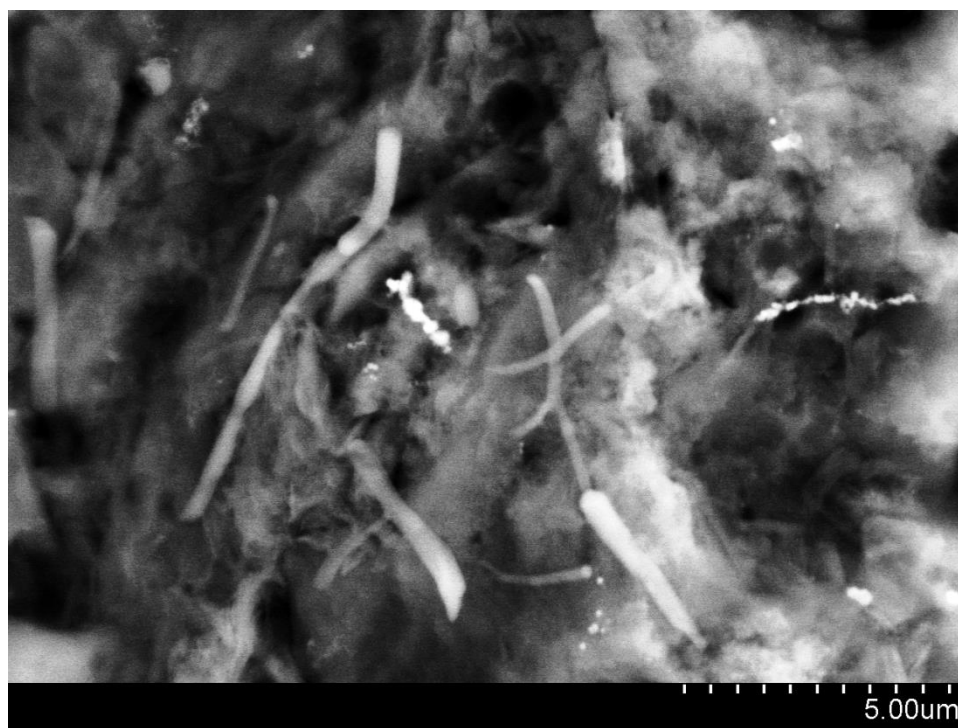


Figure 3.16: Scanning electron micrograph of Cow Rumen 1 consortium colonized cathode poised at -790mV

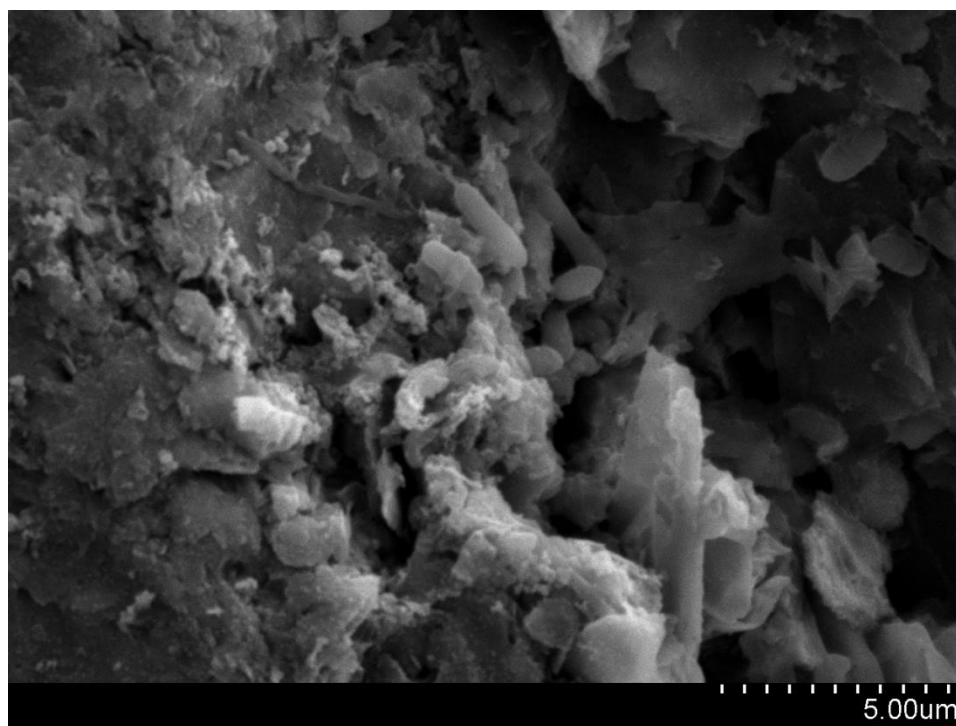


Figure 3.17 Scanning electron micrograph of Cow Rumen 1 consortium colonized cathode poised at -790mV

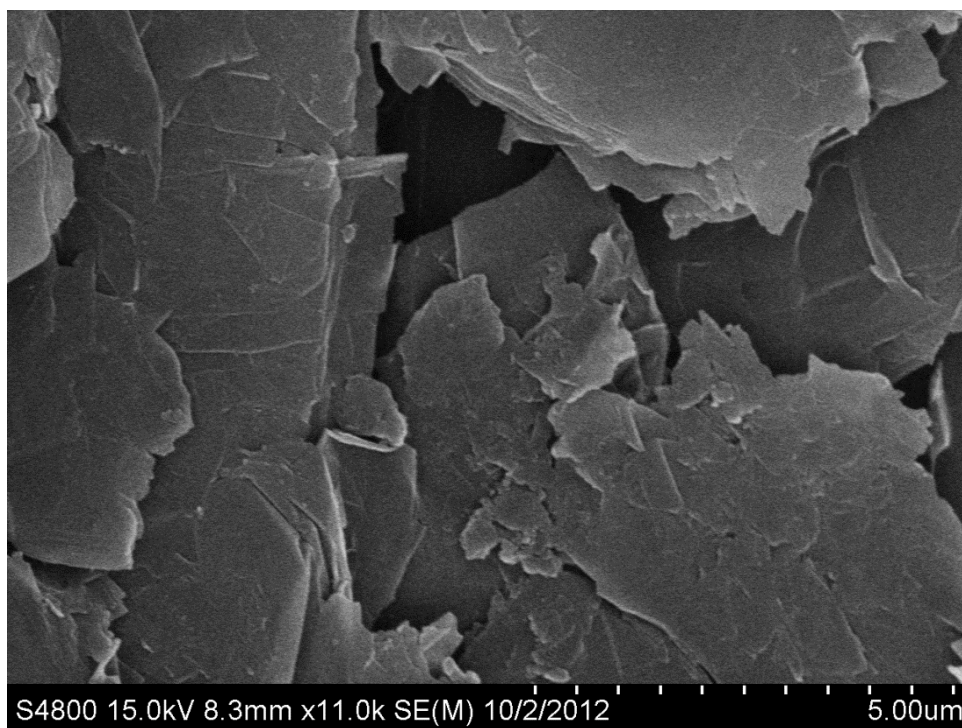


Figure 3.18 Scanning electron micrograph of a sterile abiotic cathode poised at -790mV

The MEC community composition was assessed by extracting total RNA from a functioning MEC system producing acetate in excess of 3.0 mM day^{-1} . The results of phylogenetic analysis of the total RNA provide the active portion of the consortium. During these production rates, the dominant active bacterial phyla were *Bacteroidetes*, *Firmicutes*, *Proteobacteria*, and *Spirochaetes*. At the genus level, as indicated in **figure 3.19**, an unclassified genera of the class Mollicutes accounted for nearly 40% of the active population. Other dominant genera observed at this time were Acholeplasma, Spirochaeta, and Sulfurospirillum. An unidentified genus of the family Eubacteriaceae accounted for nearly 7% of the active microbial population. The order Spingobacteriales accounted for 3.2% of the active consortium population at the order level.

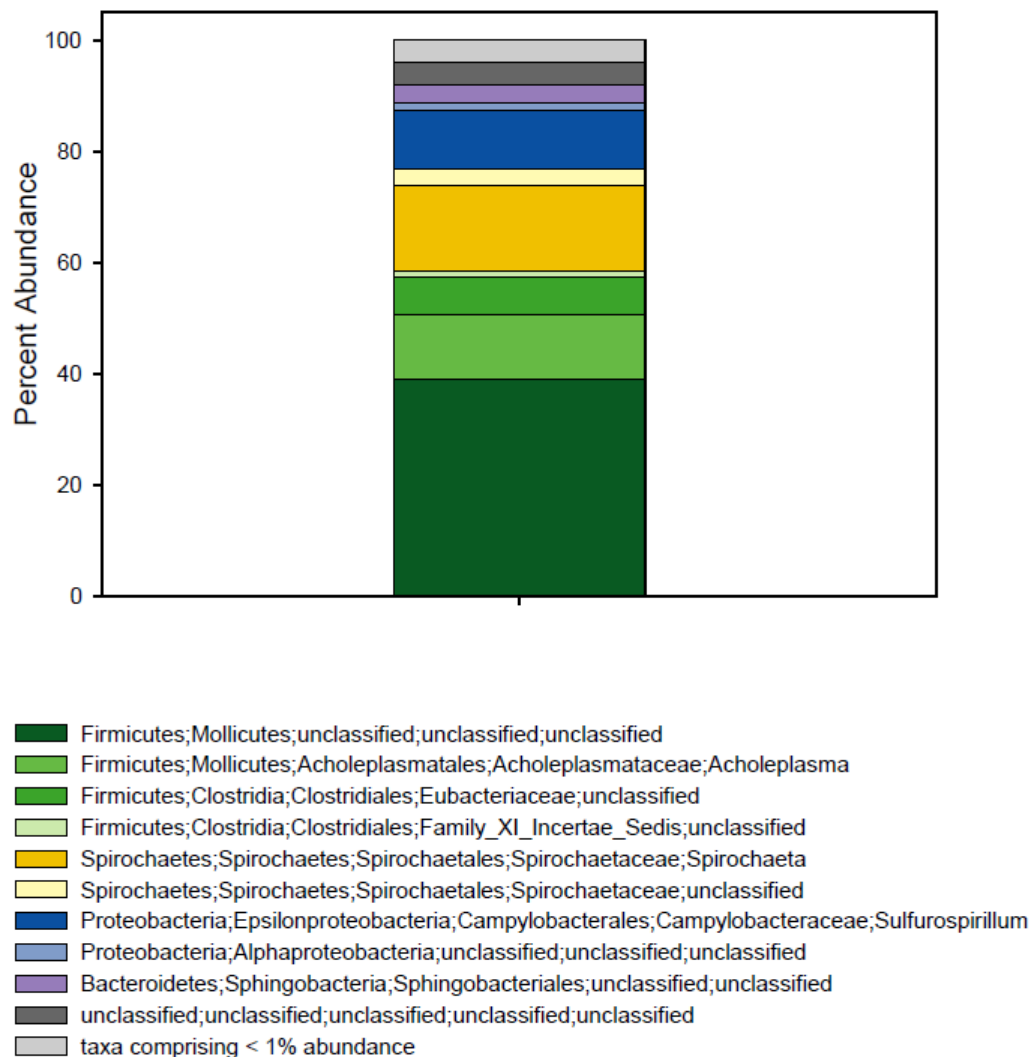


Figure 3.19: Relative abundance of active members of the cathode supernatant consortium of Cow

Rumen 1 grown at -790 mV at the genus level

To initiate isolation of the microbes within the acetogenic MEC, twelve subsets of the electroacetogenic cow rumen consortium were created through a series of serial dilutions grown in enrichment conditions. Non linear amounts of acetate production were observed with respect to dilution factor. Dilution factors receiving $1/1000^{\text{th}}$ or less of the inocula size ($1 \text{ A CR } 10^{-4}$) produced nearly 50% of the acetate as the least diluted community in the A series ($1 \text{ A CR } 10^{-1}$) of dilutions. Similar trends were

observed in the B series of dilutions were , 1B CR 10^{-4} , and 1B CR 10^{-6} dilutions yielded nearly 90% and 30% of the acetate produced by the least dilute community respectively as shown in **figure 3.20**

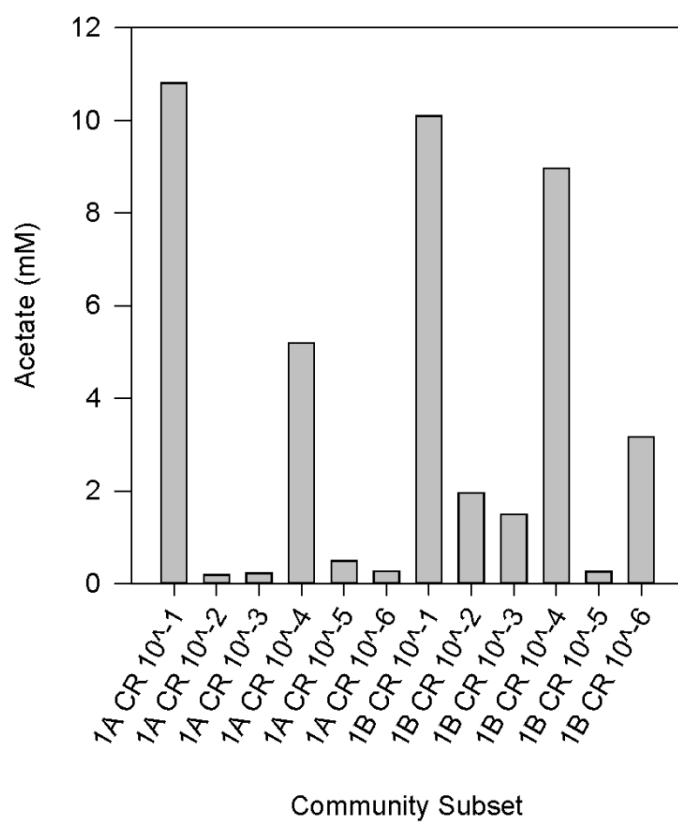


Figure 3.20: Acetate production from consortium subsets of Cow Rumen 1 grown on CO_2 and H_2

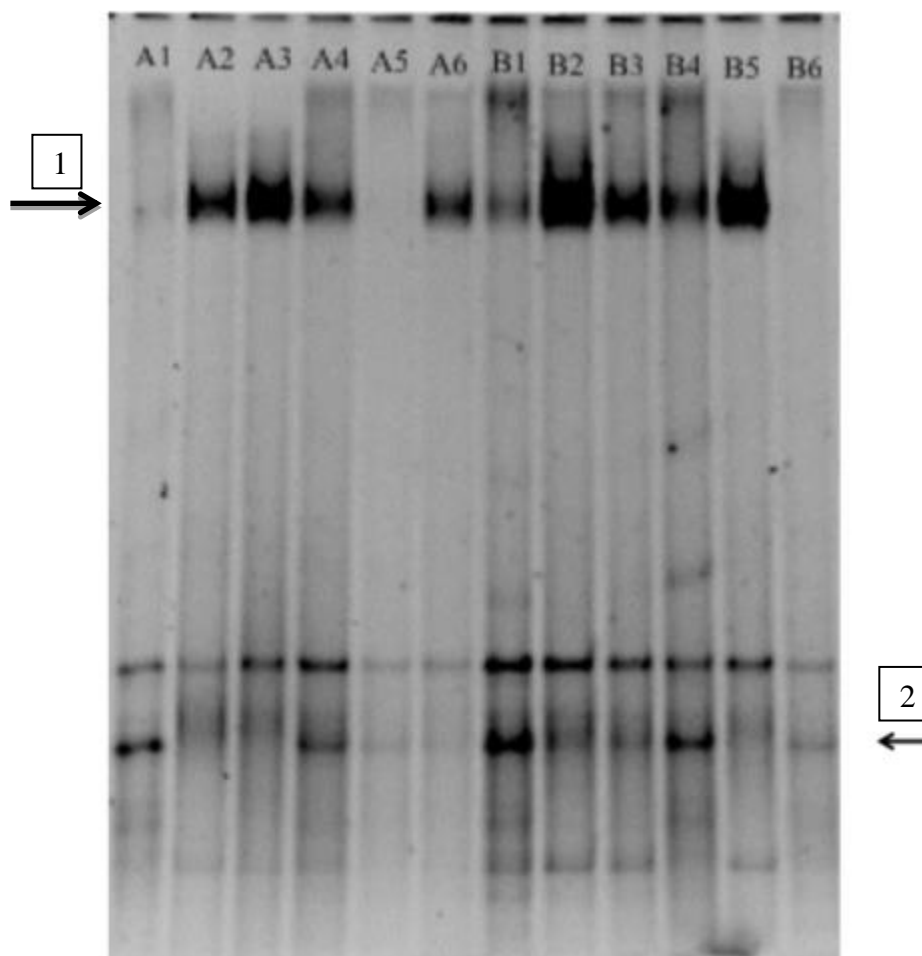


Figure 3.21: Denaturing gradient gel electrophoresis gel showing total diversity of subsets of the Cow Rumen 1 consortium. Letter at the top of each lane indicate the subset, while number indicate the diltion factor in terms of 10^{-x} .

DGGE analysis (**figure 3.21**) of the twelve consortium subsets revealed several notable differences that correlated with acetate production shown in the above **figure 3.20**. Band intensities indicated by arrow 2 show higher abundance in subsets A1, A4, B1, B4, and B6. These consortium subsets produced levels of acetate ranging from 3 to 11 mM even though the dilution factors were 10^{-1} ,

10^{-4} , and 10^{-6} . Also of note, the absence of a band in samples A1, A5, and B6, indicated by arrow 1, did not correlate with acetate production.

Based on the acetate production rates observed in **figure 3.20** community subset 1B CR 10^{-6} was selected for evaluation in an electrochemical cell to determine if the increased acetate production rates observed in the enrichment conditions would also be observable in an MEC system.

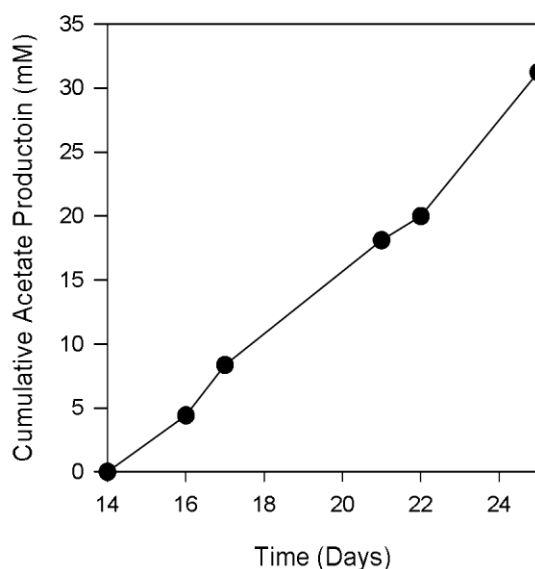


Figure 3.22: Cumulative electrochemical acetate production of Cow Rumen consortium subset 1B CR 10^{-6} grown at -790 mV. Cumulative acetate concentration (■).

Acetate production in Cow Rumen consortium 1 subset 1B 10^{-6} was approximately $3.0 \text{ mM L}^{-1} \text{ day}^{-1}$ at an applied potential of -790 mV as shown in **figure 3.22**. During the 11 day incubation the MEC system passed a total of 1826 C and reached an ending concentration of 32.5 mM acetate. Electron recovery rates with regards to acetate varied between 84 and 79% as shown in **figure 3.23**. Statistically significant differences in acetate production and coulombic efficiency were not found between the parent Cow Rumen 1 consortium and subset 1B CR 10^{-6} ($\alpha=0.05$).

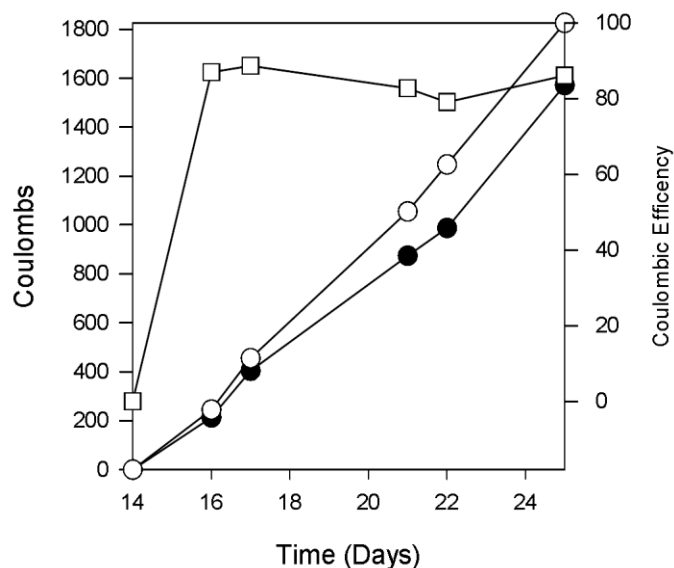


Figure 3.23: Cumulative current consumption and coulombic efficiency of Cow Rumen consortium subset 1B CR 10^{-6} grown at -790 mV. Coulombs consumed by the MEC (○). Calculated coulombs recovered in acetate (●).Coulombic efficiency (□)calculated with respect to acetate production. Coulombs consumed in an abiotic control MEC (▲)

The mechanism of bioelectrosynthetic acetate production in these cells was further assessed by alternating the provision of electrons (as reductive current flow) supplied externally by the potentiostat. **Figure 3.24** shows acetate production by an MEC that was allowed to operate and produce acetate for 36 hours. The MEC was then converted to an open circuit condition by disconnecting the cathode from the potentiostat during which time no current could flow to the cathode. During this time, no further acetate production was observed. When the cathode was re-connected at a potential of -790 mV vs. SHE was then reapplied, current consumption and acetate production both resumed promptly. The recovery rate for electrons in acetate in this experiment was between 70 and 80% (**Figure 3.25**), consistent with earlier findings shown in **Figure 3.6** and **Figure 3.7**.

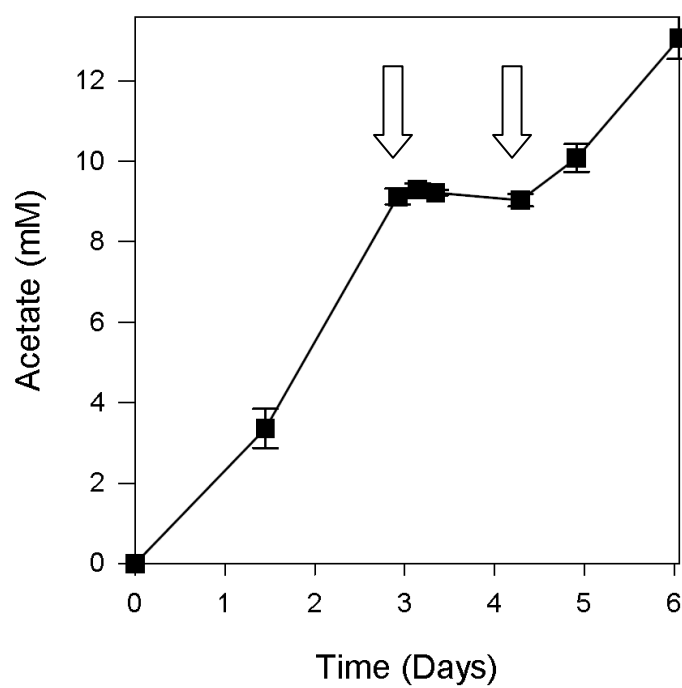


Figure 3.24 Cumulative electrochemical acetate production of Cow Rumen consortium 1 grown in the presence and absence of an applied potential of -790 mV. Arrows indicate the removal and re-application of potential. Error bars indicate standard error (n=2).

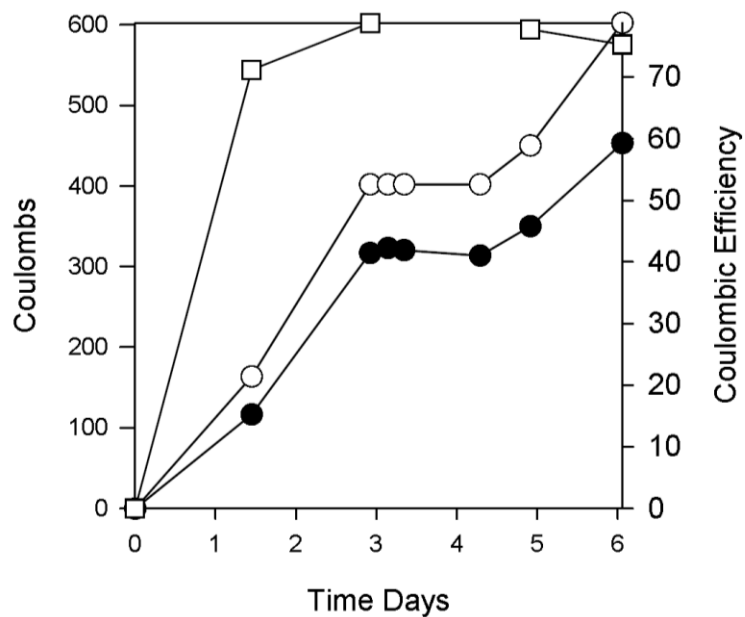


Figure 3.25 Cumulative current consumption and coulombic efficiency of Cow Rumen consortium grown in the presence and absence of an applied potential of -790 mV. Total coulombs consumed by the MEC (○). Calculated coulombs recovered in acetate (●).Coulombic efficiency (□) calculated with respect to acetate production. Error bars indicate standard error (n=2).

CHAPTER FOUR

DISCUSSION

The efficient storage of electrical energy produced by wind or solar methods is of great importance to meet peak energy demands and may be achieved through the use of microbial electrosynthesis of multiple carbon compounds such as acetate or other valuable bioproducts. The results of this project indicate that a stable microbial consortium can be an excellent catalyst to convert renewable forms of electrical energy to bioproducts of value. One of these products is the biofuel precursor acetate, which in the present work was produced autotrophically by a mixed microbial consortium derived from bovine rumen fluid growing in association with a cathode poised at -790mV vs. SHE as well as a microbial consortium derived from salt marsh sediment growing in association with a cathode poised at -590mV vs. SHE. Acetate, the sole end product observed, was produced at sustainable rates up to 3.3 mM day⁻¹ for the rumen derived inoculum. The consortium developed in this study is unique in that acetate was the sole end product produced.

Development of mixed microbial consortia capable of microbial electrosynthesis was targeted by first developing mixed consortia capable of producing acetate autotrophically via the Wood-Ljungdahl pathway. Sample sites were chosen in areas suspected to contain high levels of nonsoluble metals because a majority of the known electrotrophic organisms are capable of utilizing extracellular metals as electron donors and acceptors (Lovely and Mester, 2008). Each of the six sample sites developed the capability of producing acetate from carbon dioxide and hydrogen in a sustainable manner as shown in **Table 3.1**. The first generation of enrichments typically showed higher levels of acetate production than several of the subsequent generations, presumably this is a result of the high organic content in the sediment and rumen samples. While early enrichment consortia had minor levels of methanogenic activity, the absence of detectable levels of CH₄ in later enrichments and MEC systems indicate that methanogenic archaea were not present or were inactive in the MEC systems. Though direct measures of removing methanogenic archaea were not taken, the frequency of transfers and the omissions of a reducing solution capable of

lowering the redox potential to levels suitable for sustained methanogenesis could explain the loss of methanogenesis (Mayer and Conrad., 1990).

Of the six mixed microbial consortia obtained in this study, only two, salt marsh 1 and the cow rumen 1 enrichment communities were capable of bioelectrosynthetic production of acetate. Salt marsh 1 community produced acetate continuously for 8 medium exchanges before electrosynthetic capability was lost and not restorable. Acetate production rates were much higher in the first 50 days than subsequent days. As pH was not actively controlled in this system, the increasingly alkaline conditions could be responsible for changes in the community structure that resulted in the loss of acetate production. Furthermore, the MEC system utilized for salt marsh sediment 1 was housed in a traditional incubator. While all junctions of the MEC system were wrapped with Teflon tape to reduce the intrusion of oxygen into the cathode chamber, there exists the possibility that oxygen intrusion could also have led to the decrease and eventual loss of electroacetogenic capability. This theory is further supported by the very low Coulombic efficiency observed in the salt marsh system. Oxygen intrusion into the cathode chamber could result in the passing of electrons to oxygen, thus lowering the coulombic efficiency.

In contrast to the salt marsh sediment consortium, the cow rumen consortium was capable of sustained bioelectrosynthetic acetate production to date. Acetate production rates and Coulombic efficiencies were much higher than those measured in the salt marsh system. Lessons learned during the operation of the salt marsh system were applied to the cow rumen system. Chiefly, the cow rumen system was operated inside an anaerobic chamber to exclude oxygen intrusion, and the pH of the cathode chamber was controlled via the sparging the headspace with high purity oxygen free $\text{N}_2:\text{CO}_2$ (80:20). The impact of pH control on acetate production is most likely not related to carbon availability in the system. At a pH above 6.5 carbon in the system should be approximately 50:50 CO_2 and HCO_3^- . As the pH climbs nearer to 7.5 the ratio of CO_2 to HCO_3^- has shifted to 5:95, actually increasing the amount of carbon available to bacteria in the aqueous phase of the medium. Many genera of acetogens are known to contain high levels of carbonic anhydrase which can catalyze the conversion of HCO_3^- to CO_2 (Braus-Stromeier et al., 1997). Thus, as with the salt marsh system, the change in pH is likely shifting the microbial consortium in a manner that impacts the acetogenic subset of total population. This theory was further tested in enrichment

conditions which examined the impact of pH on total acetate yield in a sealed system. As demonstrated in **figure 3.11**, optimal production occurred at pH ranges containing higher proportions of HCO_3^- than CO_2 . Increased levels of HCO_3^- yield higher levels of carbon in the aqueous phase of the medium as CO_2 is sparingly soluble when compared to HCO_3^- at circumneutral pH.

To date, only three previous reports have described the bioelectrosynthetic production of acetate from carbon dioxide. Lovely et al. (2010) and Nevin et al. (2010, 2011) reported acetate, occasional formate, and occasional 2-oxobutyrate production by several pure cultures with a maximum production rate of 0.17 mM day^{-1} acetate observed with *Sporomusa ovata*. Recently, Marshall et al. (2012) demonstrated coincident acetate, methane, and hydrogen production at a cathode potential of -590 mV vs SHE using a mixed microbial community derived from brewery waste and grown on high surface area granular carbon electrodes. Following the addition of bromoethanesulphonic acid, a methanogenic inhibitor, Marshall et al., (2012) observed acetate and hydrogen as the sole end products. To our best knowledge, the work presented in this study represents the first mixed microbial consortium capable of producing acetate as the sole end product of electrosynthesis as hydrogen and methane were never observed during electrosynthetic growth in either the salt marsh consortium or the cow rumen consortium. Additionally, while some reports have observed acetate production rates as high as $4 \text{ mM L}^{-1} \text{ day}^{-1}$ (Marshall et al., 2012) these studies were carried out using granular graphite electrodes with high surface areas. Calculated surface areas were not presented for their systems, similar granular systems examined for possible use in this study had several times greater surface area than the electrode geometry used in the cow rumen system. Assuming normalization of acetate production per area, results from this study would mostly likely be the highest reported acetate yield per area per day to date.

To evaluate that acetate was generated from the reduction of carbon dioxide, and thus eliminate an exogenous source of carbon, isotopic labeling studies were conducted using ^{13}C -labeled bicarbonate to evaluate the conversion of carbon dioxide/bicarbonate to acetate. Quantitative transfer of the isotopic label from the carbon source to acetate provided direct evidence that acetate is the result of the bicarbonate reduction. Furthermore, these results rule out the possibility of acetate formation from stored cellular energy resulting from previous cell growth under a hydrogen headspace as has been implicated in other

acetogenic systems (Lundie et al., 1988). The longevity of the continuous production of acetate from carbon dioxide/bicarbonate without the addition of other carbon substrates also strongly suggests the acetate is produced solely from bicarbonate. To our knowledge, this study represents the first direct evidence for the flow of carbon from initial substrate, bicarbonate, through an electrosynthetic current consuming system yielding acetate. While the initial focus of isotopic labeling has targeted end product formation, the implementation of a pulse chase experiment utilized ^{13}C bicarbonate could possibly shed more light on carbon cycling in this complex consortium (Evrard et al., 2010).

To further demonstrate that electrosynthetic acetate production occurred directly from the consumption of carbon dioxide and electrical current a MEC system was operated in an alternating fashion whereby electrons were provided for a period of time, then the supply of electrons was withheld, followed by the reapplication of electrons. Acetate production was quantified during these three time periods showing that prior to removal of current the MEC systems were producing acetate at approximately 3mM day^{-1} . When operated in an open circuit configuration, acetate production ceased. When electrons were again made available, acetate production resumed almost immediately at the previous production rate. The alternating acetate production concomitant with the presence or absence of current flow provided by the potentiostat indicates an absolute requirement for these electrons and that acetate was not produced by alternative means.

Cyclic voltammetry (CV) is an electrochemical method of sweeping an applied voltage between a maximum and minimum and monitoring the resulting current flow at every potential within the scan range. In the case of MEC systems, CV is a powerful tool that can help determine the midpoint potentials of electrochemical reactions. Furthermore, CV performed on components of a biotic MEC system can reveal the means of electron transfer from the electrode to the biotic community. CV performed on biofilm containing electrodes revealed high current flow at several different applied potentials. First order integrals of the CV scan were not very telling possibly due to the low peak height observed while scanning at 2 mV/s , and additionally due to the large magnitude of double layer charging present for the MEC system which contributes to a very “fat” CV. Visual estimation of peak midpoints, however, places the midpoint of the catalytic current at roughly -0.450 mV . This observation is roughly in line with other

published values of midpoint potentials for the catalysis of carbon dioxide reduction by a mixed consortium of microbes (Marshall et al., 2012).

Having established that microbial electrosynthesis was responsible for the production of acetate, SEM images obtained from cathodes removed from MEC systems producing more than 3mM day⁻¹ acetate revealed a sporadic, thin biofilm growing in association with the cathode. Microbes were visually estimated to cover less than 10% of the total electrode surface area. This is not entirely unexpected as previously studies have reported thinner and more sporadic biofilm formation for cultures grown in electron consuming conditions on electrodes (Strycharz et al., 2008). Interestingly, there appear to be two distinct morphologies associated with the cathode. On close examination, areas of colonization of one morphology appear to not be colonized by the second morphology as areas colonized by both morphologies were not observed. It can be hypothesized that there is some level of competition or exclusions between the two dominant electrode communities; however, their role, if any, in the electrosynthetic production of acetate is currently unknown. Isolation of these two electrode dominant species could lead to a better understanding of their role electron transfer in mixed microbial communities. Ideally, follow up studies targeting transcriptomics of the electrode and supernatant communities to shed more light on the role and function of the predominant electrode communities.

The lack of detectable hydrogen accumulation in the MEC headspace is of interest and could possibly provide insight into the mechanism by which electrons are passed from an electrode to microbes in the MEC. The lack of detectable hydrogen is consistent with direct transfer of electrons from the electrode to cells where they are used to produce acetate without the intermediacy of hydrogen (Reguera et al., 2005). However, this observation does not exclude the possibility of microbially catalyzed reduction of protons to hydrogen, with subsequent acetate production via traditional anaerobic reduction. Hydrogen would not be detectable in this case if the rate of hydrogen consumption was equal to or higher than that of hydrogen production. CV performed on biocathodes emmersed in sterile growth medium provide further evidence of direct electron transfer. A distinct catalytic wave center around -450 mV is observed on biocathode scans. Catalytic current was not detected in this potential range for CV of cell free spent growth medium or sterile growth medium. Currently, sufficient data are lacking to further speculate upon the mechanisms of electron

transfer in this system; however, future studies and the use of metatranscriptomic, and possibly genetic modification methods could shed further light on the means of electron transfer.

Mixed microbial consortia are immensely complex systems of interactions between numerous organisms growing in a common environment. Over time, mixed consortia will tend to trend toward a stable equilibrium with respect to diversity, abundance, and product formation. The MEC community in this study was driven toward stability through adaptation to electrosynthetic conditions. The use of stable mixed consortia is often times desirable due to their inherent stability and robustness. The data presented thus far indicate that at least one member of the consortium used in this study was capable of receiving electrons from the cathode, either directly or indirectly. It is unknown, however, whether the electrotroph in the system was also an acetogen. Of particular interest, an unidentified genus of the family Eubacteriaceae accounted for 6.7% of the total abundance at the genus level. The family Eubacteriaceae has documented acetogenic as well as electroacetogenic function; therefore, making this family a target for future studies (Nevin et al., 2011). The order Sphingobacteriales might also play a role in the transfer of electrons from the cathode as its growth has been well documented in electrochemical systems (Zhang et al., 2012) (Nishio et al., 2010). To the authors best knowledge, the class Mollicutes, a member of the family Firmicutes, has not been previously been reported growing in association with an electrode. Thus, it is thought that their abundance in the active community has been overexpressed due to methodology associated with sample preparation prior to sequencing. Trizol was used as a chemical means of cell lysis. Mechanical means of cell lysis were not used, leading the authors of this work to believe that the high abundance of the Mollicutes stems from the fact that they are typically reported as lacking a cell wall and being bound by a plasma membrane alone (Razin, 1985).

Subsets of the Cow Rumen 1 consortium revealed several distinct rates of acetate production and consortium structures as shown in **figure 3.19** and **figure 3.20**. DGGE revealed a band (indicated by arrow 2) in **figure 3.20** that appeared to correlate with increased rates of acetate production when grown on H₂ and CO₂. Evaluations of this community subset shown in **figure 3.22** and **figure 3.23** revealed very similar results to that of the Cow Rumen 1 consortium. This result indicates that the presence of a strong acetogenic community might not directly impact electrochemical acetate production. Possibly, the

microbes able to interact directly with the electrode serve as an intermediary between the electrode surface and acetogens indicating that the electrophic organisms might be the rate limiting step in this system.

Additionally, this study was the first to utilize isotopic labeling to track the carbon present in the electrosynthetically produced acetate back to the growth substrate, bicarbonate. Furthermore, direct evidence was provided that indicated the necessity of current for electrosynthesis. While sustainable electrosynthetic production of acetate is a solid base from which to build a biofuel industry, much more research is needed to further develop this process. High end-product yields, increased electron recovery rates, and production of further reduced end products such as alcohols are required in order for this technology to be brought to practice. Mixed microbial consortia represent a broad range of metabolisms that have the possibility to produce very diverse end products; however, sustainable alcohol production by a mixed microbial consortium has yet to be reported. Perhaps, in the future, engineered consortia can be design to tailor an electrosynthetic process to a specific end product.

REFERENCES

- Ahn, Youngho, and Bruce E. Logan. "Effectiveness of domestic wastewater treatment using microbial fuel cells at ambient and mesophilic temperatures." *Bioresource technology* 101.2 (2010): 469-475.
- Aulenta, Federico, et al. "Electron transfer from a solid-state electrode assisted by methyl viologen sustains efficient microbial reductive dechlorination of TCE." *Environmental science & technology* 41.7 (2007): 2554-2559.
- Bond, Daniel R., et al. "Electrode-reducing microorganisms that harvest energy from marine sediments." *Science* 295.5554 (2002): 483-485.
- Bond, Daniel R., and Derek R. Lovley. "Electricity production by *Geobacter sulfurreducens* attached to electrodes." *Applied and environmental microbiology* 69.3 (2003): 1548-1555.
- Braus-Stromeier, Susanna A., et al. "Carbonic anhydrase in *Acetobacterium woodii* and other acetogenic bacteria." *Journal of bacteriology* 179.22 (1997): 7197-7200.
- Breznak, John A. "Acetogenesis from carbon dioxide in termite guts." *Acetogenesis* (1994): 303-330.
- Childers, Susan E., Stacy Ciufo, and Derek R. Lovley. "Geobacter metallireducens accesses insoluble Fe (III) oxide by chemotaxis." *Nature* 416.6882 (2002): 767-769.
- Das, Amaresh, and Lars G. Ljungdahl. "Electron-transport system in acetogens." *Biochemistry and Physiology of Anaerobic Bacteria* (2003): 191-204.
- Deng, Qian, et al. "Power generation using an activated carbon fiber felt cathode in an upflow microbial fuel cell." *Journal of Power Sources* 195.4 (2010): 1130-1135.
- Drake, Harold L. "Acetogenesis, acetogenic bacteria, and the acetyl-CoA "Wood/Ljungdahl" pathway: past and current perspectives." *Acetogenesis* (1994): 3-60.
- Doukov, Tzanko I., et al. "A Ni-Fe-Cu center in a bifunctional carbon monoxide dehydrogenase/acetyl-CoA synthase." *Science* 298.5593 (2002): 567-572.
- Emde, Rainer, and Bernhard Schink. "Enhanced propionate formation by *Propionibacterium freudenreichii* subsp. *freudenreichii* in a three-electrode amperometric culture system." *Applied and environmental microbiology* 56.9 (1990): 2771-2776.
- Farnleitner, Andreas H., et al. "Simultaneous Detection and Differentiation of *Escherichia coli* Populations from Environmental Freshwaters by Means of Sequence Variations in a Fragment of the β -d-Glucuronidase Gene." *Applied and Environmental Microbiology* 66.4 (2000): 1340-1346.
- Fichot, Erin B., and R. Sean Norman. "Microbial phylogenetic profiling with the Pacific Biosciences sequencing platform." *Microbiome* 1.1 (2013): 10.
- Gerhard Gottschalk. *Bacterial Metabolism*. Springer, 1986.
- Gregory, Kelvin B., Daniel R. Bond, and Derek R. Lovley. "Graphite electrodes as electron donors for anaerobic respiration." *Environmental microbiology* 6.6 (2004): 596-604.

- Gottwald, Mechthild, et al. "Presence of cytochrome and menaquinone in *Clostridium formicoaceticum* and *Clostridium thermoaceticum*." *Journal of Bacteriology* 122.1 (1975): 325.
- Hawthorne, John Russell, and Douglas Creese Harrison. "Cytochrome c as a carrier with the glucose dehydrogenase system." *Biochemical Journal* 33.10 (1939): 1573.
- Heise, R., V. Müller, and G. Gottschalk. "Sodium dependence of acetate formation by the acetogenic bacterium *Acetobacterium woodii*." *Journal of Bacteriology* 171.10 (1989): 5473-5478.
- Hernandez, M. E., and D. K. Newman. "Extracellular electron transfer." *Cellular and molecular life sciences* 58.11 (2001): 1562-1571.
- Hoffert, Martin I., et al. "Advanced technology paths to global climate stability: energy for a greenhouse planet." *Science* 298.5595 (2002): 981-987.
- Hu, Shou-Ih, E. Pezacka, and H. G. Wood. "Acetate synthesis from carbon monoxide by *Clostridium thermoaceticum*. Purification of the corrinoid protein." *Journal of Biological Chemistry* 259.14 (1984): 8892-8897.
- Hugenholtz, Jeroen.,D. Mack Ivey, and Lars G. Ljungdahl. "Carbon monoxide-driven electron transport in *Clostridium thermoautotrophicum* membranes." *Journal of Bacteriology* 169.12 (1987): 5845-5847.
- Hugenholtz, Jeroen and Lars G. Ljungdahl. "Electron transport and electrochemical proton gradient in membrane vesicles of *Clostridium thermoautotrophicum*." *Journal of Bacteriology* 171.5 (1989): 2873-2875.
- Jones, J. G., and B. M. Simon. "Interaction of acetogens and methanogens in anaerobic freshwater sediments." *Applied and Environmental Microbiology* 49.4 (1985): 944-948.
- Joblin, K. N. "Ruminal acetogens and their potential to lower ruminant methane emissions." *Crop and Pasture Science* 50.8 (1999): 1307-1314.
- Kiely, Patrick D., et al. "Long-term cathode performance and the microbial communities that develop in microbial fuel cells fed different fermentation endproducts." *Bioresource Technology* 102.1 (2011): 361-366.
- Krichevsky, I. R., and J. S. Kasarnovsky. "Thermodynamical calculations of solubilities of nitrogen and hydrogen in water at high pressures." *Journal of the American Chemical Society* 57.11 (1935): 2168-2171.
- Kuroda, M., T. Watanabe, and Y. Umedu. "Simultaneous oxidation and reduction treatments of polluted water by a bio-electro reactor." *Water Science and Technology* 34.9 (1996): 101-108.
- Liu, Shi, and Joseph M. Suflita. "H₂-CO₂-dependent anaerobic O-demethylation activity in subsurface sediments and by an isolated bacterium." *Applied and Environmental Microbiology* 59.5 (1993): 1325-1331.

- Lovley, Derek R., and Tünde Mester. "Proteome of *Geobacter sulfurreducens* grown with Fe (III) oxide or Fe (III) citrate as the electron acceptor." *Biochimica et Biophysica acta* 2008 (1784): 1935-1941.
- Lovley, DerekR. "Long-range electron transport to Fe (III) oxide via pili with metallic-like conductivity." *Biochemical Society Transactions* 40.6 (2012): 1186-1190.
- Ljungdhal, L. G. "The autotrophic pathway of acetate synthesis in acetogenic bacteria." *Annual Reviews in Microbiology* 40.1 (1986): 415-450.
- Ljungdahl, Lars G. "The acetyl-CoA pathway and the chemiosmotic generation of ATP during acetogenesis." *Acetogenesis. Chapman & Hall, New York, NY*(1994): 63-87.
- Lundie Jr, L. L., et al. "Energy-dependent, high-affinity transport of nickel by the acetogen *Clostridium thermoaceticum*." *Journal of Bacteriology* 170.12 (1988): 5705-5708.
- Marshall, Christopher W., et al. "Electrosynthesis of Commodity Chemicals by an Autotrophic Microbial Community." *Applied and Environmental Microbiology*(2012).
- Marsili, Enrico, et al. "Shewanella secretes flavins that mediate extracellular electron transfer." *Proceedings of the National Academy of Sciences* 105.10 (2008): 3968-3973.
- Matthews, Rowena G. "Cobalamin-dependent methyltransferases." *Accounts of Chemical Research* 34.8 (2001): 681-689.
- Peter Mayer, H., and Ralf Conrad. "Factors influencing the population of methanogenic bacteria and the initiation of methane production upon flooding of paddy soil." *FEMS Microbiology Letters* 73.2 (1990): 103-111.
- Mehanna, Maha, et al. "Microbial electrodialysis cell for simultaneous water desalination and hydrogen gas production." *Environmental Science & Technology* 44.24 (2010): 9578-9583.
- Menon, Saurabh, and Stephen W. Ragsdale. "Evidence that carbon monoxide is an obligatory intermediate in anaerobic acetyl-CoA synthesis." *Biochemistry* 35.37 (1996): 12119-12125.
- Meyer, O., K. Frunzke, and G. Mörsdorf. "Biochemistry of the aerobic utilization of carbon monoxide." *Microbial Growth on C 1* (1993): 433-459.
- Müller, V., and Gerhard Gottschalk. "The sodium ion cycle in acetogenic and methanogenic bacteria: generation and utilization of a primary electrochemical sodium ion gradient." *Acetogenesis. Chapman & Hall, New York, NY* (1994): 127-156.
- Müller, V., et al. "Molecular and cellular biology of acetogenic bacteria." *Strict and Facultative Anaerobes: Medical and Environmental Aspects* (2004): 251-281.
- Nevin, Kelly P., et al. "Microbial electrosynthesis: feeding microbes electricity to convert carbon dioxide and water to multicarbon extracellular organic compounds." *MBio* 1.2 (2010).

- Nevin, Kelly P., et al. "Electrosynthesis of organic compounds from carbon dioxide is catalyzed by a diversity of acetogenic microorganisms." *Applied and Environmental Microbiology* 77.9 (2011): 2882-2886.
- Nishio, Koichi, Kazuhito Hashimoto, and Kazuya Watanabe. "Light/electricity conversion by a self-organized photosynthetic biofilm in a single-chamber reactor." *Applied Microbiology and Biotechnology* 86.3 (2010): 957-964.
- Park, D. H., and JGI Zeikus. "Utilization of Electrically Reduced Neutral Red by *Actinobacillus succinogenes*: Physiological Function of Neutral Red in Membrane-Driven Fumarate Reduction and Energy Conservation." *Journal of Bacteriology* 181.8 (1999): 2403-2410.
- Ragsdale, S. W., P. A. Lindahl, and E. Münck. "Mössbauer, EPR, and optical studies of the corrinoid/iron-sulfur protein involved in the synthesis of acetyl coenzyme A by *Clostridium thermoaceticum*." *Journal of Biological Chemistry* 262.29 (1987): 14289-14297.
- Ragsdale, Stephen W. "Nickel and the carbon cycle." *Journal of Inorganic Biochemistry* 101.11 (2007): 1657-1666.
- Ragsdale, Stephen W., and Elizabeth Pierce. "Acetogenesis and the Wood–Ljungdahl pathway of CO₂ fixation." *Biochimica et Biophysica Acta (BBA)-Proteins & Proteomics* 1784.12 (2008): 1873-1898.
- Razin, Shmuel. "Molecular biology and genetics of mycoplasmas (Mollicutes)." *Microbiological Reviews* 49.4 (1985): 419.
- Reguera, Gemma, et al. "Extracellular electron transfer via microbial nanowires." *Nature* 435.7045 (2005): 1098-1101.
- Roberts, Leslie. "9 Billion?." *Science* 333.6042 (2011): 540-543.
- Sakakibara, Yutaka, and Masao Kuroda. "Electric prompting and control of denitrification." *Biotechnology and Bioengineering* 42.4 (1993): 535-537.
- Schlegel, H. G., and R. Lafferty. "Growth of 'Knallgas' bacteria (*Hydrogenomonas*) using direct electrolysis of the culture medium." (1965): 308-309.
- Strycharz, Sarah M., et al. "Graphite electrode as a sole electron donor for reductive dechlorination of tetrachlorethene by *Geobacter lovleyi*." *Applied and Environmental Microbiology* 74.19 (2008): 5943-5947.
- Strycharz, Sarah M., et al. "Reductive dechlorination of 2-chlorophenol by *Anaeromyxobacter dehalogenans* with an electrode serving as the electron donor." *Environmental Microbiology Reports* 2.2 (2010): 289-294.
- Tanner, Ralph S., et al. "A phylogenetic analysis of anaerobic eubacteria capable of synthesizing acetate from carbon dioxide." *Current Microbiology* 7.3 (1982): 127-132.

- Thrash, J. Cameron, et al. "Electrochemical stimulation of microbial perchlorate reduction." *Environmental Science & Technology* 41.5 (2007): 1740-1746.
- Thrash, J. Cameron, and John D. Coates. "Review: direct and indirect electrical stimulation of microbial metabolism." *Environmental Science & Technology* 42.11 (2008): 3921-3931.
- United States Energy Information Administration. *Annual Energy Outlook*. N.p.: n.p., 2012. N. pag. Web. 21 Mar. 2013.
- Von Canstein, Harald, et al. "Secretion of flavins by Shewanella species and their role in extracellular electron transfer." *Applied and Environmental Microbiology* 74.3 (2008): 615-623.
- Zhang, Guodong, et al. "Efficient electricity generation from sewage sludge using biocathode microbial fuel cell." *Water Research* 46.1 (2012): 43-52.